CHAPTER

11 Solids with Elliptic Inclusions

In practice, we do not expect the inclusions to be of an exact canonical shape. The models considered in the previous two chapters are adequate for the heterogeneous solids with equiaxial inclusions where the mean radius is the only length parameter of inclusion. When the inclusion's shape deviates considerably from the equiaxial/circular one, we need an additional length parameter to quantify it. In this case, an ellipse (also possessing two length parameters) appears to be more a appropriate model shape. In particular, an infinitely thin elliptic hole is a convenient model of the straight crack. Therefore, an extension of our approach to the solids with elliptic inclusions seems worthwhile in both theoretical and practical aspects.

The analytical solutions for the interacting elliptic inclusions are limited to a few. A certain progress is observed in the conductivity problem where the multipole expansion solution has been obtained for the finite [231] and periodic [232] arrays of elliptical cylinders. A series of solutions of the elasticity problem for two identical elliptic inclusions [143] is written in terms of real potentials. Derived by accurate matching of the elastic fields in the matrix and inclusions, an infinite set of equations is rather involved and thus difficult to use. The complex potentials in 2D linear elasticity are advantageous in comparison with their real-valued counterparts [160] provided the appropriate potential functions were taken[1]. The complete solutions for a finite array of elliptic inclusions in the plane [116] and half-plane [117] have been obtained by combining the multipole expansion method with the Kolosov-Muskhelishvili technique of complex potentials. This approach has been further developed and applied to the evaluation of the stress intensity factors [120] and effective stiffness [121] of cracked solids.

11.1 Single Elliptic Inclusion in an Inhomogeneous Far Field

11.1.1 Problem Statement and Form of Solution

Consider an infinite isotropic elastic solid with a single, elliptic in cross-section, long fiber embedded. We assume the external load to be applied in a way that the stress

[1] It is appropriate to mention here the work [210] where a special form of complex potentials has been suggested and the solution of the single elliptic hole problem has been obtained in a much more simple and elegant way as compared with the standard conformal mapping technique.

Micromechanics of Composites. http://dx.doi.org/10.1016/B978-0-12-407683-9.00011-4

field does not vary in the fiber axis direction. In this case, the problem can be stated as 2D (plane strain or plane stress formulation), which, in turn, enables using the method of complex potentials. To describe the geometry of the problem, we introduce first the Cartesian coordinate frame Ox_1x_2 so that its origin coincides with the centroid of ellipse whereas the Ox_1 and Ox_2 axes are directed along the major and minor axes of the ellipse. An aspect ratio of the ellipse is $e = l_2/l_1$, where l_1 and l_2 are the major and minor, respectively, semi-axes of the ellipse. Another derivative geometric parameter to be used in subsequent analysis is the inter-foci distance $2d$, where $d = \sqrt{l_1^2 - l_2^2}$.

Alongside with conventional complex variable $z = x_1 + \mathrm{i}x_2$, we will use the "elliptic" complex variable $\xi = \zeta + \mathrm{i}\eta$ introduced (e.g., [207]) as

$$z = \omega(\xi) = d\cosh\xi. \tag{11.1}$$

In fact, Eq. (11.1) defines an elliptic coordinate frame with ζ and η as "radial" and "angular" coordinates, respectively. In particular, the coordinate curve $\zeta = \zeta_0$ is an ellipse specified by the condition

$$\zeta_0 = \ln\left(\frac{l_1 + l_2}{d}\right) = \frac{1}{2}\ln\left(\frac{1+e}{1-e}\right), \tag{11.2}$$

see Figure 11.1. It is important that the points of matrix-elliptic inclusion interface are the functions of angular coordinate η only. This fact makes the complex variable ξ particularly useful in the problems formulated on domains with elliptic boundaries/interfaces.

The complex displacement $u = u_1 + \mathrm{i}u_2$ is expressed in terms of complex potentials φ and ψ by Eq. (9.78) of Section 9.6. Cartesian components of the associated with u stress tensor $\boldsymbol{\sigma}$ are given by Eq. (9.79). The displacement u and normal traction τ_n are assumed to be continuous at the elliptic matrix-inclusion interface L: So, $\zeta = \zeta_0$:

$$[[u]]_L = 0; \quad [[\tau_n]]_L = 0, \tag{11.3}$$

where $[[f]]_L$ means a jump of f through the interface L: So, $[[u]]_L = \left(u^{(0)} - u^{(1)}\right)_L$ and upper indices "0" and "1" refer to matrix and inclusion, respectively. Also,

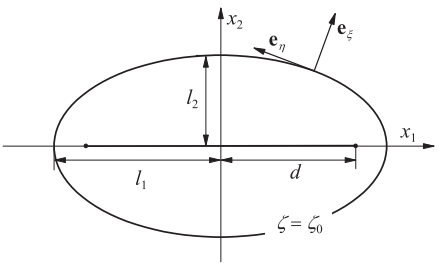

FIGURE 11.1

Geometry of the problem.

$\mu = \mu_0, \nu = \nu_0$ in the matrix and $\mu = \mu_1, \nu = \nu_1$ in the inclusion. Fulfilling the conditions Eq. (11.3) is greatly simplified by working with curvilinear, normal, and tangential to interface $\zeta = \zeta_0$ components of the displacement $\mathbf{u} = u_\zeta \mathbf{e}_\zeta + u_\eta \mathbf{e}_\eta$ and traction $\mathbf{T}_n = \sigma_{\zeta\zeta}\mathbf{e}_\zeta + \sigma_{\zeta\eta}\mathbf{e}_\eta$ vectors. In complex form,

$$u = u_\zeta + \mathrm{i}u_\eta; \quad \tau_n = \sigma_{\zeta\zeta} - \mathrm{i}\sigma_{\zeta\eta}.$$

Their expression in terms of complex potentials is [160]:

$$\begin{aligned} u_\zeta + \mathrm{i}u_\eta &= \frac{\overline{\omega'(\xi)}}{|\omega'(\xi)|}\left[\varkappa\varphi(z) - (z-\overline{z})\overline{\varphi'(z)} - \overline{\psi(z)}\right]; \\ \sigma_{\zeta\zeta} - \mathrm{i}\sigma_{\zeta\eta} &= 2\mu\left\{\varphi'(z) + \overline{\varphi'(z)}\right. \\ &\quad \left. - \frac{\omega'(\xi)}{\overline{\omega'(\xi)}}\left[(\overline{z}-z)\varphi''(z) - \varphi'(z) + \psi'(z)\right]\right\}, \end{aligned} \tag{11.4}$$

where, as follows from Eq. (11.1), $\omega'(\xi) = dz/d\xi = d\sinh\xi$.

As always, the key to success is an appropriate choice of the potential functions φ and ψ. The straightforward (but, definitely, not the best) way is to write them as [143]

$$\varphi = \sum_n A_n \upsilon^{-n}, \quad \psi = \sum_n B_n \upsilon^{-n}, \tag{11.5}$$

where A_n and B_n are the complex coefficients and $\upsilon = \exp\xi = z/d \pm \sqrt{(z/d)^2 - 1}$. It appears, however, that the potentials Eq. (11.5) lead to are rather cumbersome in resolving the system. Moreover, in this case, even the Eshelby-type problem, known to possess a closed-form solution, is given by an infinite series [143]. An alternate, advantageous form of ψ [116] is

$$\begin{aligned} \psi &= \psi_0 - \psi_1, \quad \psi_0 = \sum_n B_n \upsilon^{-n}, \\ \psi_1 &= \frac{\sinh\zeta_0}{\sinh\xi}\left(\frac{\upsilon}{\upsilon_0} - \frac{\upsilon_0}{\upsilon}\right)\sum_n n A_n \upsilon^{-n}, \end{aligned} \tag{11.6}$$

where $\upsilon_0 = \exp(\zeta_0)$. Introduced by this way ψ Eq. (11.6) is an analytical function of z. The functions $\frac{\upsilon^n}{\sinh\xi} = \frac{d}{n}\frac{d\upsilon^n}{dz}$ obtained by differentiation of υ^n with respect to z can be viewed as an alternate basis function in Eq. (11.5). The potentials φ_i and ψ_i for solution in the inclusion S_1 are also given by Eqs. (11.5) and (11.6), with replacing A_n and B_n to C_n and D_n, respectively; C_n and D_n are also the complex coefficients, which also are to be found from the interface condition Eq. (11.3).

11.1.2 Displacement and Traction at the Elliptic Interface

The displacement u Eq. (9.78) contains the derivative $\varphi'(z) = d\varphi/dz$: We rewrite it as

$$\varphi'(z) = \frac{d\varphi}{d\xi}\frac{d\xi}{dz} = \frac{\varphi'(\xi)}{\omega'(\xi)}. \tag{11.7}$$

On the ellipse $\zeta = \zeta_0$,

$$(z - \overline{z}) = d \sinh \zeta_0 \left(t - t^{-1} \right), \tag{11.8}$$

where $t = \exp(\mathrm{i}\eta)$ and $t^n = \exp(\mathrm{i}n\eta)$ is the Fourier harmonic of angular variable η. In these notations, the second term of Eq. (9.78) becomes

$$(z - \overline{z})\overline{\varphi'(z)} = -\frac{d \sinh \zeta_0}{\overline{\omega'\left(\xi\right)}} \left(t - t^{-1} \right) \sum_n n \overline{A_n} \exp\left(-n\zeta_0\right) t^n.$$

On the other hand, the second term in Eq. (11.6) for $\zeta = \zeta_0$ is

$$\psi_1 = \frac{d \sinh \zeta_0}{\omega'(\xi)} \sum_n n A_n \left(t - t^{-1} \right) \exp(-n\zeta_0) t^{-n}. \tag{11.9}$$

It is clear that these terms cancel each other in Eq. (9.78) and, thus, one obtains

$$u|_L = \varkappa\varphi - \overline{\psi_0} = \sum_n \left(\varkappa A_n \upsilon^{-n} - \overline{B_n \upsilon^{-n}} \right). \tag{11.10}$$

Now, we consider the traction vector τ_n in the form of Eq. (11.4). Taking Eq. (11.7) into account yields

$$\frac{(\sigma_{\zeta\zeta} - \mathrm{i}\sigma_{\zeta\eta})}{2\mu} = \frac{\varphi'}{\omega'} + \frac{\overline{\varphi'}}{\overline{\omega'}} - \frac{\omega'}{\overline{\omega'}} \left[(\overline{\omega} - \omega) \frac{\varphi'' - \frac{\omega}{\omega'}\varphi'}{(\omega')^2} - \frac{\varphi'}{\omega'} + \frac{\psi'}{\omega'} \right],$$

where the argument ξ is omitted for brevity and differentiation is made with respect to ξ. We transform it to

$$\frac{(\sigma_{\zeta\zeta} - i\sigma_{\zeta\eta})}{2\mu} = \frac{\overline{\varphi'} - \psi_0'}{\overline{\omega'}} + \frac{1}{\omega'\overline{\omega'}} \left[(\omega' + \overline{\omega'})\varphi' + \omega'\psi_1' - (\overline{\omega} - \omega) \left(\varphi'' - \frac{\omega}{\omega'}\varphi' \right) \right]. \tag{11.11}$$

It follows from Eqs. (11.7–11.9) that for $\zeta = \zeta_0$

$$\psi_1 = \frac{(\overline{\omega} - \omega)}{\omega'}\varphi'$$

being substituted into Eq. (11.11), it gives

$$\frac{(\sigma_{\zeta\zeta} - \mathrm{i}\sigma_{\zeta\eta})}{2\mu} = \frac{\overline{\varphi'} - \psi_0'}{\overline{\omega'}} + \frac{1}{\omega'\overline{\omega'}} \left[(\omega' + \overline{\omega'})\varphi' - (\overline{\omega} - \omega)\varphi'' + \omega'\psi_1' + \omega\psi_1 \right]. \tag{11.12}$$

Now, differentiation of ψ_1 Eq. (11.6) with respect to ξ yields

$$\omega'\psi_1' + \omega\psi_1 = -d\sinh\zeta_0 \sum_n nA_n[(n-1)\,t - (n+1)\,t^{-1}] \times \exp(-n\zeta_0)\,t^{-n}. \tag{11.13}$$

On the other hand, we combine (11.8) with

$$\omega' + \overline{\omega'} = d\sinh\zeta_0\left(t + t^{-1}\right)$$

to prove that

$$(\omega' + \overline{\omega'})\varphi' - (\overline{\omega} - \omega)\varphi'' = d\sinh\zeta_0 \sum_n nA_n \exp(-n\zeta_0)\,t^{-n}\left[n\left(t - t^{-1}\right) - \left(t + t^{-1}\right)\right]$$

is equal to Eq. (11.13) with opposite sign. Thus, the whole expression in square brackets in Eq. (11.11) equals zero and we obtain, by taking conjugate of Eq. (11.12),

$$\omega'\frac{\tau_n}{2\mu}\bigg|_{\zeta=\zeta_0} = \varphi' - \overline{\psi_0'} = \sum_n (-n)\left(A_n\upsilon^{-n} - \overline{B_n\upsilon^{-n}}\right). \tag{11.14}$$

As seen, Eqs. (11.10) and (11.13) are quite analogous to Eqs. (10.52) and (10.52) of Section 10.4. The equivalence of Eqs. (9.78) and (10.49) was discussed already in Chapter 10: In what follows, we keep using the representation of Eq. (9.78).

11.1.3 Formal Solution

With φ Eq. (11.5) and ψ Eq. (11.6), the expression of u and τ_n (11.4) at the interface $\zeta = \zeta_0$ simplifies greatly. By virtue of Eq. (11.10), the first condition of Eq. (11.3) is equivalent to

$$[[\varkappa\varphi - \overline{\psi_0}]]_L = 0.$$

In explicit form,

$$\sum_n \upsilon_0^{-n}\left(\varkappa_0 A_n t^{-n} - \overline{B_n}t^n\right) = \sum_n \upsilon_0^{-n}\left(\varkappa_1 C_n t^{-n} - \overline{D_n}t^n\right),$$

where $\varkappa_i = \varkappa(\nu_i)$. By equating the coefficients of equal Fourier harmonics $t^n = \exp(\mathrm{i}n\eta)$ we obtain an infinite set of linear algebraic equations

$$\varkappa_0 A_n\upsilon_0^{-n} - \overline{B}_{-n}\upsilon_0^n = \varkappa_1 C_n\upsilon_0^{-n} - \overline{D}_{-n}\upsilon_0^n.$$

The second condition of Eq. (11.3) is equivalent to

$$\left[\left[2\mu\left(\varphi' - \overline{\psi_0'}\right)\right]\right]_L = 0.$$

By applying the same procedure we get another set of linear equations:

$$A_n \upsilon_0^{-n} + \overline{B}_{-n} \upsilon_0^n = \frac{\mu_1}{\mu_0} (C_n \upsilon_0^{-n} + \overline{D}_{-n} \upsilon_0^n).$$

It is advisable, for computational purpose, to introduce the scaled variables $\widetilde{A}_n = A_n \upsilon_0^{-n}$, and so on. In these variables,

$$\begin{aligned} \varkappa_0 \widetilde{A}_n - \overline{\widetilde{B}}_{-n} &= \varkappa_1 \widetilde{C}_n - \overline{\widetilde{D}}_{-n}, \\ \widetilde{A}_n + \overline{\widetilde{B}}_{-n} &= \frac{\mu_1}{\mu_0} (\widetilde{C}_n + \overline{\widetilde{D}}_{-n}) \quad \left(-\infty < n < \infty\right). \end{aligned} \tag{11.15}$$

Equation (11.15) is remarkably simple (see, for comparison, [143]) that clearly indicates rational choice of the potential functions (11.6).

The solution we derived is a general one. In each specific case, the redundant degrees of freedom should be excluded by imposing the constraints drawn from physical considerations. One of them is the regularity of the displacement field inside the inclusion, i.e., $u^{(1)}$ is continuous and finite for $z \in S_1$. It means that the Laurent series expansions of corresponding complex potentials contain the only non-negative powers of z. The following relations between C_n and D_n, with positive and negative index n,

$$C_n = C_{-n}; \quad D_n = D_{-n} + 2n \sinh(2\zeta_0) C_{-n} \quad (n > 0) \tag{11.16}$$

provide regularity of $u^{(1)}$ and $\sigma^{(1)}$ inside the inclusion. To prove it, we will show that the separate terms in Eq. (9.78) are the polynomials of variables x_1 and x_2. Provided $C_n = C_{-n}$, φ Eq. (11.5) is written as

$$\varphi\left(z\right) = \sum_n C_n (\upsilon^n + \upsilon^{-n}) = 2 \sum_n C_n \cosh\left[n \operatorname{Arccosh}\left(\frac{z}{d}\right)\right]. \tag{11.17}$$

Remarkably, the hyperbolic cosine standing on the right-hand side of Eq. (11.17) is exactly the nth degree Chebyshev polynomial of complex variable z/d. It is clear that its derivative with respect to z as well as the product $\left(z - \overline{z}\right) \overline{\varphi'}$ obeys the regularity condition.

Also, we transform ψ_0 Eq. (11.6) with aid of Eq. (11.16) to

$$\psi_0 = \sum_n \left[D_{-n} (\upsilon^n + \upsilon^{-n}) + 2nC_n \sinh 2\zeta_0 \upsilon^{-n}\right].$$

Here, the first term is, likewise Eq. (11.17), the polynomial of degree n. The difference

$$\begin{aligned} \psi_1 - 2 \sum_n nC_n \sinh 2\zeta_0 \upsilon^{-n} = \sum_n nC_n \frac{\sinh \zeta_0}{\sinh \xi} \Big[&\left(\upsilon^{n-1} - \upsilon^{-(n-1)}\right) \upsilon_0 \\ &- \left(\upsilon^{n+1} - \upsilon^{-(n+1)}\right) / \upsilon_0 \Big] \end{aligned}$$

is also a polynomial of z that follows directly from the identity

$$\frac{d}{dz} \left(\upsilon^n + \upsilon^{-n}\right) = n \frac{\upsilon^n - \upsilon^{-n}}{d \sinh \xi}.$$

Thus, the whole $\psi = \psi_0 - \psi_1$ and, hence, u Eq. (9.78) is regular provided the coefficients C_n and D_n, with positive and negative indices, obey the conditions Eq. (11.16).

As to a solution in the matrix domain, we split it into a sum $u^{(0)} = u_{\text{far}} + u_{\text{dis}}$, where u_{far} is the incident, or far field, whereas u_{dis} describes disturbance field induced by the inclusion. It is expected that $u_{\text{dis}} \to 0$ as $|z| \to \infty$. The corresponding potentials φ and ψ are also divided onto singular and regular parts

$$\varphi = \varphi_s + \varphi_r, \quad \psi = \psi_s + \psi_r.$$

The explicit form of φ_s and ψ^s is given by Eqs. (11.5) and (11.6), respectively, where we keep the terms with negative powers of υ only to provide a vanishing of the disturbance field at infinity, so

$$A_n = B_n \equiv 0 \quad \text{for } n \leqslant 0. \tag{11.18}$$

On the contrary, u_{far} is assumed to be regular, with the potentials

$$\varphi_r = \sum_n a_n \upsilon^{-n}, \tag{11.19}$$

$$\psi_r = \sum_n \left[b_n - 2n a_n \frac{\sinh \zeta_0}{\sinh \xi} \sinh(\xi - \zeta_0) \right] \upsilon^{-n},$$

where a_n and b_n necessarily comply with Eq. (11.16). For example, the uniform far strain tensor $\mathbf{E} = \{E_{ij}\}$ induces the linear displacement field

$$u_{\text{far}} = (E_{11} x_1 + E_{12} x_2) + \mathrm{i}(E_{12} x_1 + E_{22} x_2). \tag{11.20}$$

It takes the form of Eq. (9.78) with the potentials Eq. (11.19), where the series coefficients

$$a_{-1} = \frac{d}{4} \frac{E_{11} + E_{22}}{(\varkappa_0 - 1)}; \tag{11.21}$$

$$b_{-1} = a_{-1} \upsilon_0^{-2} + \frac{d}{4}(E_{22} - E_{11} + 2\mathrm{i} E_{12});$$

a_1 and b_1 are given by Eq. (11.16) and all other a_n and b_n for $n \neq \pm 1$ are equal to zero. In the case of the far stress tensor $\mathbf{S} = \{S_{ij}\}$ prescribed, the expression is quite similar:

$$a_{-1} = \frac{d}{16\mu_0}(S_{11} + S_{22}); \tag{11.22}$$

$$b_{-1} = a_{-1} \upsilon_0^{-2} + \frac{d}{8\mu_0}(S_{22} - S_{11} + 2\mathrm{i} S_{12}).$$

The displacement u_{far} and corresponding traction τ_n^r at the interface $\zeta = \zeta_0$ take the form of Eqs. (11.10) and (11.14), respectively. Applying the procedure analogous to that described above gives us an infinite linear system

$$\begin{gathered} \varkappa_0 A_n \upsilon_0^{-n} - \overline{B}_{-n} \upsilon_0^n + \varkappa_0 a_n \upsilon_0^{-n} - \overline{b}_{-n} \upsilon_0^n = \varkappa_1 C_n \upsilon_0^{-n} - \overline{D}_{-n} \upsilon_0^n; \\ A_n \upsilon_0^{-n} + \overline{B}_{-n} \upsilon_0^n + a_n \upsilon_0^{-n} + \overline{b}_{-n} \upsilon_0^n = \widetilde{\mu}_1 \left(C_n \upsilon_0^{-n} + \overline{D}_{-n} \upsilon_0^n \right), \end{gathered} \tag{11.23}$$

where $\widetilde{\mu}_1 = \mu_1 / \mu_0$.

In the single-inclusion problem under study, we assume u_{far} (or, the same, a_n and b_n) to be known. In this case, Eq. (11.23) together with Eqs. (11.16) and (11.18) form a closed set of linear algebraic equations possessing a unique solution. By substituting Eqs. (11.16) and (11.18) into Eq. (11.23) we come to resolving the linear system

$$\begin{aligned}
\varkappa_0 A_n - \varkappa_1 C_n + (\overline{D_n} - 2n\sinh 2\zeta_0 \overline{C_n})\upsilon_0^{2n} &= -\varkappa_0 a_n + \overline{b_{-n}}\upsilon_0^{2n}; \quad (11.24)\\
\overline{B_n} + \varkappa_1 C_n \upsilon_0^{2n} - \overline{D_n} &= \varkappa_0 a_{-n}\upsilon_0^{2n} - \overline{b_n};\\
A_n - \frac{\mu_1}{\mu_0} C_n - \widetilde{\mu}_1(\overline{D_n} - 2n\sinh 2\zeta_0 \overline{C_n})\upsilon_0^{2n} &= -a_n - \overline{b_{-n}}\upsilon_0^{2n};\\
\overline{B_n} - \widetilde{\mu}_1 C_n \upsilon_0^{2n} - \widetilde{\mu}_1 \overline{D_n} &= -a_{-n}\upsilon_0^{2n} - \overline{b_n};\\
n &= 1, 2, \ldots
\end{aligned}$$

with the unknowns A_n, B_n, C_n, and D_n ($n > 0$) and with the coefficients a_n and b_n entering the right-hand side vector. For the Eshelby-type problem with the uniform far strain $\mathbf{E}$ or stress field $\mathbf{S}$, these coefficients are given by Eq. (11.21) or Eq. (11.22), respectively. The corresponding resolving system Eq. (11.24) consists of four equations for $n = 1$ determining uniquely the coefficients A_1, B_1, C_1, and D_1.

11.1.4 Stress Intensity Factor

The above solution is valid for $0 < e < 1$. We consider the limiting case $e \to 0$ where the ellipse degenerates into the cut $|x_1| \leqslant d$ in the complex plane (another limit $e \to 1$ where an ellipse becomes a circle, is trivial). By letting $\mu_1 = 0$ we get a straight crack, the stress field around which is known to possess a singularity in the crack tips. In the linear fracture mechanics, the stress intensity factor (SIF) defined as

$$K_{\text{I}} + \text{i}K_{\text{II}} = \lim_{z\to d} \sqrt{2\pi(z-d)}\left(\sigma_{22} + \text{i}\sigma_{12}\right)$$

is generally accepted to quantify the stress field near the tip of crack. No problems arise with taking this limit in the above solution: For $e \to 0$ we have, from Eq. (11.2), $\zeta_0 \to 0$ and $\upsilon_0 \to 1$. After simple algebra, one obtains an expression of complex SIF $K = K_{\text{I}} + \text{i}K_{\text{II}}$ in terms of A_n and B_n:

$$K = -2\mu_0\sqrt{\frac{\pi}{d}}\sum_{n=1}^{\infty} n\left(A_n + \overline{B_n}\right),$$

valid for arbitrary, not necessarily uniform, far load.

11.2 Re-Expansion Formulas for the Elliptic Solid Harmonics

Let the position of the arbitrarily taken (say, with index p) elliptic inclusion with interfoci length $2D_p$ in the complex plane, related to the global Cartesian coordinate frame Ox_1x_2, be given by the complex number $Z_p = X_{1p} + \text{i}X_{2p}$ defining the

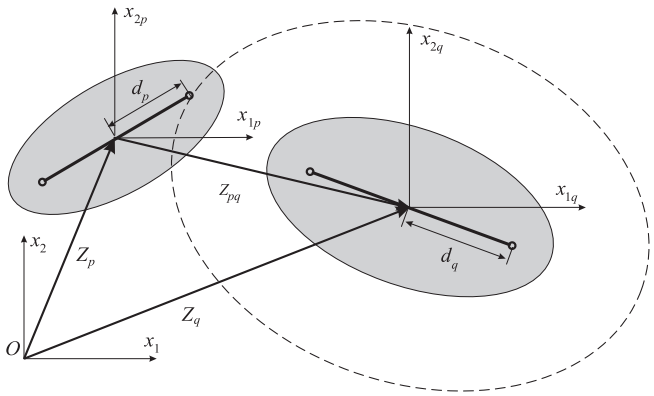

FIGURE 11.2

Global and local coordinate systems.

midpoint O_p and inclination angle Θ_p ($\|\Theta_p\| \leqslant \pi/2$) between the interfoci cut and positive direction of the Ox_1 axis. We introduce the local coordinate frame $O_p x_{1p} x_{2p}$ so that its origin coincides with O_p whereas the $O_p x_{1p}$ and $O_p x_{2p}$ axes are parallel to the corresponding axes of the global coordinate frame. The global $z = x_1 + \mathrm{i}x_2$ and local $z_p = x_{1p} + \mathrm{i}x_{2p}$ variables are related by $z = z_p + Z_p$, see Figure 11.2. We define the inclusion-related elliptic coordinates $\xi_p = \zeta_p + \mathrm{i}\eta_p$ by the formula

$$z_p = d_p \omega(\xi_p) = d_p \cosh(\xi_p),$$

where $d_p = D_p \exp(\mathrm{i}\Theta_p)$. Also,

$$\upsilon_p = \exp(\xi_p) = z_p/d_p \pm \sqrt{\left(z_p/d_p\right)^2 - 1} \quad (\mathrm{Re}\,\upsilon_p > 0).$$

The inverse formula is $z_p = \frac{1}{2} d_p (\upsilon_p + 1/\upsilon_p)$.

In the multi-inclusion problem, one has to re-expand the pth inclusion-related "irregular" elliptic harmonics $(\upsilon_p)^{-n}$ ($n > 0$) in a vicinity of another, say, qth inclusion. For this purpose, we derive the re-expansion formula

$$\upsilon_p^{-n} = \sum_m \eta_{nm}^{pq} \upsilon_q^{-m} \quad (n \geqslant 1), \tag{11.25}$$

where the expansion coefficients $\eta_{nm}^{pq} = \eta_{nm}\left(Z_{pq}, d_p, d_q\right)$ and $Z_{pq} = Z_q - Z_p$. In the particular case of two collinear identical elliptic coordinate frames with $D_p = D_q$ and $\mathrm{Im}\, Z_{pq} = 0$, η_{nm} has been found [143] as an infinite integral of the product of the Bessel functions. For the arbitrarily placed, equally oriented elliptic coordinate frames with the same semi-foci parameter $D_p = D_q$, Yardley et al. [231] expressed η_{nk}^{pq} by means of hypergeometric function and have suggested the convenient for numerical evaluation formula. In our notations, it has the form

$$\eta_{nm}^{pq} = \frac{1}{\pi} \int_0^{\pi} (\upsilon_p)^{-n}|_{\zeta_q = 0} \cos(m\eta_q) d\eta_p \quad (m \geqslant 1). \tag{11.26}$$

This formula provides a clear insight into the meaning of the coefficients η_{nm}^{pq} being nothing else but the Fourier expansion coefficients of $\left(\upsilon_p\right)^{-n}$ in terms of η_q. The series expansions of η_{nm}^{pq} [116] are valid for the arbitrary, not necessarily equal, values of D_p and D_q. It is straightforward to prove that all the above mentioned formulas of η_{nm}^{pq} are valid, within their convergence area, for the arbitrarily oriented elliptic coordinate frames provided we replace the real-valued parameters D_p and D_q with their complex counterparts, d_p and d_q. Note, a combination of Eqs. (11.47) and (11.48) gives analogous to [143] integral representation of the expansion coefficients

$$\eta_{nm}^{pq} = n\mathrm{i}^{m-n}\int_0^\infty \beta^{-1} J_n\left(d_p\beta\right) J_m\left(d_q\beta\right)\exp\left(\mathrm{i}\beta Z_{pq}\right) d\beta, \tag{11.27}$$

free of the above mentioned geometric restrictions.

However, the computational effort of the η_{nm} evaluation from either Eq. (11.26) or Eq. (11.27) is quite considerable. An efficiency of numerical algorithm can be improved by using two series expansions of η_{nm} [116]. The first one is based on three easy-to-derive expansions:

$$\upsilon_p^{-n} = \sum_{k=0}^{\infty} \frac{n}{n+2k}\binom{n+2k}{k}\left(\frac{d_p}{2z_p}\right)^{n+2k} \quad \left(\left|z_p\right| > d_p\right); \tag{11.28}$$

$$z_p^{-n} = \sum_{k=0}^{\infty} \binom{n+k-1}{k}(-1)^k Z_{pq}^{-(n+k)} z_q^k \quad \left(\left|z_q\right| < \left|Z_{pq}\right|\right); \tag{11.29}$$

and

$$\left(\frac{2z_q}{d_q}\right)^n = \sum_{k=0}^{n}\binom{n}{k}\upsilon_q^{2k-n}.$$

The last formula is free of geometric restrictions. Consecutive application of these formulas gives the following expression of η_{nm} in Eq. (11.25):

$$\eta_{nm}^{pq} = nd_p^n(-1)^m\sum_{l=0}^{\infty} d_q^{2l+m} M_{nml}\left(d_p, d_q\right)\frac{\left(n+m+2l-1\right)!}{\left(2Z_{pq}\right)^{n+m+2l}}, \tag{11.30}$$

where

$$M_{nml}\left(d_p, d_q\right) = \sum_{k=0}^{l}\frac{\left(d_p/d_q\right)^{2k}}{k!(l-k)!(k+n)!(m+l-k)!}. \tag{11.31}$$

Note that $\eta_{nm} = \eta_{n,-m}$: It follows directly from the fact that υ_p^{-n} is regular in a vicinity of Z_q and hence the expansion coefficients must comply with Eq. (11.16). The drawback of Eq. (11.30) is the geometric restrictions narrowing its convergence area. Two of them, namely $|z_p| > d_p$ and $|z_q| < |Z_{pq}|$ came from Eqs. (11.28) and (11.29), respectively; $|Z_{pq}| > (d_p + d_q)$ is an additional condition providing series convergence in Eq. (11.30).

To fix this problem, we rewrite Eq. (11.30) in a somewhat modified form. Namely, we transform it with aid of the analogous to Eq. (11.29) formula

$$\left(\frac{d_{pq}}{2Z_{pq}}\right)^n = \sum_{k=0}^{\infty}(-1)^k \binom{n+k-1}{k} \upsilon_{pq}^{-(n+2k)},$$

where $d_{pq} = d_p + d_q$ and $\upsilon_{pq} = Z_{pq}/d_{pq} + \sqrt{\left(Z_{pq}/d_{pq}\right)^2 - 1}$. After an appropriate change of summation order, we come to[2]

$$\eta_{nm}^{pq} = (-1)^m n \left(\frac{d_p}{d_{pq}}\right)^n \sum_{j=0}^{\infty} \upsilon_{pq}^{-(n+m+2j)} \sum_{l=0}^{j} \frac{(-1)^{j-l}}{(j-l)!} \left(\frac{d_p}{d_{pq}}\right)^{m+2l} M_{nml}\left(d_p, d_q\right) \frac{n+m+l+j-1)!}{(j-l)!}. \tag{11.32}$$

The series Eq. (11.25) with the coefficients Eq. (11.32) converges within an ellipse centered in Z_q with inter-foci distance d_{pq} and passing the pole of the pth elliptic coordinate frame closest to Z_q (the dashed ellipse in Figure 11.2), which is sufficient to solve any two non-overlapping ellipses. For a comprehensive convergence study of the expansion Eq. (11.25), see [231,232].

For the well-separated inclusions, Eq. (11.32) simplifies to Eq. (11.30). Moreover, in the case $d_p = d_q$ Eq. (11.31) reduces to

$$M_{nml} = \frac{(n+m+l+1)_l}{l!(n+l)!(m+l)!},$$

where $(n)_m$ is the Pochhammer's symbol. The obtained Eq. (11.30) is simple and easy to compute. Therefore, when one solves for many inclusions, the computational effort-saving strategy is to apply either Eq. (11.26) or Eq. (11.32) to the nearest neighbors whereas a contribution from the more distant inclusions is evaluated using Eq. (11.30).

Finally, we mention two useful consequences of Eq. (11.25). The first of them is obtained by differentiation of Eq. (11.25) with respect to z_q:

$$\frac{\upsilon_p^{-n}}{\sinh \xi_p} = \frac{d_p}{d_q} \sum_m \frac{m}{n} \eta_{nm}^{pq} \frac{\upsilon_q^{-m}}{\sinh \xi_q}.$$

Another derivative of Eq. (11.25), this time with respect to Z_{pq}, is

$$\frac{\upsilon_p^{-n}}{\sinh \xi_p} = \sum_m \mu_{nm}^{pq} \upsilon_q^{-m}, \tag{11.33}$$

[2]This derivation does not pretend to be mathematically rigorous. A general and theoretically substantiated derivation of the re-expansion formulas has been suggested in [81]. The final result, however, coincides with Eq. (11.32) obtained by means of standard algebra.

where

$$\mu_{nm}^{pq} = \mu_{nm}\left(Z_{pq}, d_p, d_q\right) = \frac{d_p}{n}\frac{\partial}{\partial Z_{pq}}\eta_{nm}^{pq}.$$

In order to evaluate the coefficients μ_{nm}^{pq}, the following two formulas are used. The first formula

$$\mu_{nm}^{pq} = -\frac{2n}{\pi d_p}\int_0^{\pi}\left.\frac{(\upsilon_p)^{-n}}{(\upsilon_p - 1/\upsilon_p)}\right|_{\zeta_q=0}\cos(m\eta_q)d\eta_p$$

is analogous to Eq. (11.26) and applies to the closely placed inclusions whereas the second one,

$$\mu_{nm}^{pq} = -2n\left(-1\right)^m\left(\frac{d_p}{2}\right)^n\sum_{l=0}^{\infty}\left(\frac{d_q}{2}\right)^{m+2l}M_{nml}\frac{\Gamma(n+m+2l+1)}{(Z_{pq})^{n+m+2l+1}} \tag{11.34}$$

is preferable for the well-separated inclusions.

11.3 Finite Array of Inclusions

Now, we proceed to a piece-homogeneous plane containing a finite number N of non-overlapping elliptic inclusions S_p with boundary L_p, semi-axes l_{1p} and l_{2p}, and elastic moduli μ_p and ν_p $(1 \leqslant p \leqslant N)$. The centroid of the pth ellipse lies in the point $Z_p = X_{1p} + \mathrm{i}X_{2p}$. For simplicity sake, we assume all ellipses to be equally oriented: hence, $\Theta_p = 0$ and $d_p = D_p$. Also, we introduce local Cartesian coordinate frames $O_p x_{1p} x_{2p}$ centered in Z_p. The local coordinates of different frames are related by $z_p = Z_{pq} + z_q$, where $z_p = x_{1p} + \mathrm{i}x_{2p}$ and $Z_{pq} = Z_q - Z_p$. The inclusion-related local curvilinear coordinates $\xi_p = \zeta_p + \mathrm{i}\eta_p$ are defined, by analogy with Eq. (11.1), as $z_p = d_p \cosh\xi_p$. In these variables, geometry of pth inclusion can be alternatively defined by a pair of parameters (ζ_{p0}, d_p), where $d_p = \sqrt{\left(l_{1p}\right)^2 - \left(l_{2p}\right)^2}$. At the matrix-inclusion interface $\zeta_p = \zeta_{p0}$, the perfect bonding

$$[[u]]_{L_p} = 0; \quad [[\tau_n]]_{L_p} = 0 \quad (1 \leqslant p \leqslant N) \tag{11.35}$$

is assumed. The stress in and around the inclusions is induced by the far field u_{far}: we assume it in the form of Eq. (11.20).

Due to linearity of the problem, the solution for a multiply connected matrix domain is written as the superposition sum

$$u^{(0)} = u_{\mathrm{far}}(z) + u_{\mathrm{dis}}(z) = u_{\mathrm{far}}(z) + \sum_{p=1}^{N} u_s^{(p)}(z - Z_p), \tag{11.36}$$

where $u_s^{(p)}$ is a disturbance induced by the pth inclusion: $\left|u_s^{(p)}\right| \to 0$ for $|z| \to \infty$. The corresponding complex potentials $\varphi_s^{(p)}$ and $\psi_s^{(p)}$ are again taken in the form Eqs. (11.5) and (11.6), resepectively. By analogy with Eq. (11.18), $A_n^{(p)} = B_n^{(p)} = 0$ for $n \leqslant 0$.

Note that the separate terms of the sum in Eq. (11.36) are written in variables of different coordinate frames. In order to fulfil the interface conditions Eq. (11.35) for, say, qth inclusion in a way exposed above, we need to expand $u^{(0)}$ locally, in variables of a given local coordinate frame. Our aim is to transform

$$u_s^{(p)}\left(z_p\right) = \varkappa_0 \varphi_s^{(p)}\left(z_p\right) - \left(z_p - \overline{z}_p\right)\overline{\varphi_s^{(p)\prime}\left(z_p\right)} - \overline{\psi_s^{(p)}\left(z_p\right)}, \tag{11.37}$$

where

$$\begin{aligned}\varphi_s^{(p)} &= \sum_{n=0}^{\infty} A_n^{(p)} \upsilon_p^{-n}, \quad \psi_s^{(p)} = \psi_{0s}^{(p)} - \psi_{1s}^{(p)} \\ &= \sum_{n=0}^{\infty}\left[B_n^{(p)} - 2nA_n^{(p)}\frac{\sinh\zeta_{p0}}{\sinh\xi_p}\sinh(\xi_p - \zeta_{p0})\right]\upsilon_p^{-n},\end{aligned}$$

into $u_r^{(p)(q)}$, written in the same form as $u_s^{(p)}$ but in qth coordinate frame, namely

$$u_r^{(p)(q)} = \varkappa_0 \varphi_r^{(p)(q)}\left(z_q\right) - \left(z_q - \overline{z}_q\right)\overline{\varphi_r^{(p)(q)\prime}\left(z_q\right)} - \overline{\psi_r^{(p)(q)}\left(z_q\right)}, \tag{11.38}$$

with

$$\begin{aligned}\varphi_r^{(p)(q)} &= \sum_n a_n^{pq}\upsilon_q^{-n}, \quad \psi_r^{(p)(q)} = \psi_{0r}^{(p)(q)} - \psi_{1r}^{(p)(q)} \\ &= \sum_n\left[b_n^{pq} - 2na_n^{pq}\frac{\sinh\zeta_{q0}}{\sinh\xi_q}\sinh(\xi_q - \zeta_{q0})\right]\upsilon_q^{-n}.\end{aligned} \tag{11.39}$$

For this purpose, we employ the above derived re-expansion formulas for the complex potentials. By applying Eq. (11.25) to $\varphi_s^{(p)}$, we obtain

$$\varphi_s^{(p)} = \sum_{n=0}^{\infty} A_n^{(p)}\upsilon_p^{-n} = \sum_n a_n^{pq}\upsilon_q^{-n} = \varphi_r^{(p)(q)}, \tag{11.40}$$

from where

$$a_n^{pq} = \sum_{m=1}^{\infty} A_m^{(p)}\eta_{mn}^{pq}. \tag{11.41}$$

With a_n^{pq} taken in the form of Eq. (11.41) the first terms in Eqs. (11.37) and (11.38) coincide, $\varkappa_0\varphi_s^{(p)} = \varkappa_0\varphi_r^{(p)(q)}$.

The determination of b_n^{pq} is somewhat more involved. From Eq. (11.40) we conclude that $\varphi_s^{(p)\prime}(z_p) = \varphi_r^{(p)(q)\prime}(z_q)$ and thus the second term in Eq. (11.37) can be transformed as

$$\left(z_p - \overline{z}_p\right)\varphi_s^{(p)\prime} = \left(Z_{pq} - \overline{Z_{pq}}\right)\varphi_r^{(p)(q)\prime} + \left(z_q - \overline{z}_q\right)\varphi_r^{(p)(q)\prime}.$$

To provide $u_s^{(p)} = u_r^{(p)(q)}$, we determine b_n^{pq} in Eq. (11.39) from

$$\psi_s^{(p)} = \psi_r^{(p)(q)} + \left(Z_{pq} - \overline{Z_{pq}}\right) \varphi_r^{(p)(q)\prime}. \tag{11.42}$$

To this end, all the terms in Eq. (11.42) should be expanded into a series of υ_q. The simplest thing is $\psi_{0s}^{(p)}$: likewise $\varphi_s^{(p)}$ Eqs. (11.40) and (11.41), we write

$$\psi_{0s}^{(p)} = \sum_{n=1}^{\infty} B_n^{(p)} \upsilon_p^{-n} = \sum_n \left(\sum_{m=1}^{\infty} B_m^{(p)} \eta_{mn}^{pq} \right) \upsilon_q^{-n}.$$

Next, we re-group $\psi_{1s}^{(p)}$ as

$$\psi_{1s}^{(p)} = \sum_{n=1}^{\infty} n A_n^{(p)} \left[\left(1 - \upsilon_{p0}^{-2}\right) \upsilon_p^{-n} - \frac{1}{2} \left(\upsilon_{p0} - \upsilon_{p0}^{-1}\right)^2 \frac{\upsilon_p^{-(n+1)}}{\sinh \xi_p} \right], \tag{11.43}$$

where $\upsilon_{p0} = \exp(\zeta_{p0})$.

With the aid of Eqs. (11.25) and (11.33), ψ_{1p}^{s} is expanded into

$$\psi_{1s}^{(p)} = \sum_n \left\{ \sum_{m=1}^{\infty} m A_m^{(p)} \left[\left(1 - \upsilon_{p0}^{-2}\right) \eta_{mn}^{pq} - \frac{1}{2} \left(\upsilon_{p0} - \upsilon_{p0}^{-1}\right)^2 \mu_{m+1,n}^{pq} \right] \right\} \upsilon_q^{-n},$$

where μ_{mn}^{pq} are the re-expansion coefficients in Eq. (11.33). Similarly to Eq. (11.43), $\psi_{1r}^{(p)(q)}$ is re-arranged to

$$\begin{aligned} \psi_{1r}^{(p)(q)} = {} & \left(1 - \upsilon_{q0}^{-2}\right) \sum_n n a_n^{pq} \upsilon_q^{-n} \\ & + \left(\upsilon_{q0} - \upsilon_{q0}^{-1}\right)^2 \sum_{n=1}^{\infty} n a_n^{pq} \frac{\upsilon_q^{n+1} - \upsilon_q^{-(n+1)}}{\upsilon_q - \upsilon_q^{-1}}. \end{aligned}$$

By applying the formula

$$\frac{\upsilon^{n+1} - \upsilon^{-(n+1)}}{\upsilon - \upsilon^{-1}} = \sum_{k=0}^{n} \upsilon^{2k-n}$$

and Eq. (11.41), we get

$$\begin{aligned} \psi_{1r}^{(p)(q)} = {} & \sum_n \left\{ \sum_{m=1}^{\infty} A_m^{(p)} \left[\left(\upsilon_{q0}^{-2} - 1\right) |n| \eta_{m|n|}^{pq} \right.\right. \\ & \left.\left. + \left(\upsilon_{q0} - \upsilon_{q0}^{-1}\right)^2 \sum_{k=0}^{\infty} (|n| + 2k) \eta_{m,|n|+2k}^{pq} \right] \right\} \upsilon_q^{-n}. \end{aligned}$$

Transformation of the last term $\left(\overline{Z}_{pq} - Z_{pq}\right)\varphi_r^{(p)(q)\prime}$ follows the same way and yields

$$\varphi_{1r}^{(p)(q)\prime} = \frac{2}{d_q}\sum_n \left\{\sum_{m=1}^{\infty} A_m^{(p)}\left[\sum_{k=0}^{\infty}(|n|+1+2k)\eta_{m,|n|+1+2k}^{pq}\right]\right\}\upsilon_q^{-n}.$$

Collecting, finally, all the expansions gives us the following b_n^{pq} expression for $n < 0$:

$$\begin{aligned} b_n^{pq} = &\sum_{m=1}^{\infty} B_m^{(p)}\eta_{mn}^{pq} + \sum_{m=1}^{\infty} A_m^{(p)}\left\{\frac{m}{2}\left(\upsilon_{p0} - \upsilon_{p0}^{-1}\right)^2\mu_{m+1,n}^{pq}\right. \\ &+\left[n\left(\upsilon_{q0}^{-2}-1\right) - n\left(1-\upsilon_{p0}^{-2}\right)\right]\eta_{mn}^{pq} + \left(\upsilon_{q0}-\upsilon_{q0}^{-1}\right)^2\sum_{k=1}^{\infty}(2k-n)\eta_{m,2k-n}^{pq} \\ &\left.+\frac{2}{d_q}\left(\overline{Z}_{pq} - Z_{pq}\right)\sum_{k=0}^{\infty}(2k+1-n)\eta_{m,2k+1-n}^{pq}\right\}. \end{aligned} \tag{11.44}$$

For $n > 0$, in accordance with Eq. (11.16),

$$b_n^{pq} = b_{-n}^{pq} + n\left(\upsilon_{q0}^2 - \upsilon_{q0}^{-2}\right)a_n^{pq}.$$

Now, we come back to Eq. (11.36) and write

$$\sum_{p=1}^{N} u_s^{(p)}(z_p) = u_s^{(q)}(z_q) + u_r^{(q)}(z_q),$$

where $u_r^{(q)}(z_q) = \sum_{p\neq q} u_r^{(p)(q)}(z_q)$ is given by Eqs. (11.38) and (11.39) with replace $\varphi_r^{(p)(q)}$ to $\varphi_r^{(q)} = \sum_{p\neq q}\varphi_r^{(p)(q)}$, $\psi_r^{(p)(q)}$ to $\psi_r^{(q)} = \sum_{p\neq q}\psi_r^{(p)(q)}$. Also,

$$a_n^{(q)} = \sum_{p\neq q} a_n^{pq}, \quad b_n^{(q)} = \sum_{p\neq q} b_n^{pq}. \tag{11.45}$$

No problems arise with the linear term in (11.36):

$$u_{\text{far}}(z) = U_q + u_{\text{far}}(z_q),$$

where $U_q = (X_{1q}E_{11} + X_{2q}E_{12}) + \mathrm{i}(X_{1q}E_{12} + X_{2q}E_{22})$ is the constant; $u_{\text{far}}(z_q)$ adds to Eq. (11.45) a few extra terms defined by Eq. (11.21) and thus, the problem has been reduced to that considered in Section 11.1.

The resolving set of equations is:

$$\begin{gathered}
\varkappa_0 A_n^{(q)} - \varkappa_q C_n^{(q)} + \left(\overline{D_n^{(q)}} - 2n\sinh 2\zeta_{q0}\overline{C_n^{(q)}}\right)\upsilon_{q0}^{2n} = -\varkappa_0 a_n^{(q)} + \overline{b_{-n}^{(q)}}\upsilon_{q0}^{2n}; \\
\overline{B_n^{(q)}} + \varkappa_q C_n^{(q)}\upsilon_{q0}^{2n} - \overline{D_n^{(q)}} = \varkappa_0 a_{-n}^{(q)}\upsilon_{q0}^{2n} - \overline{b_n^{(q)}}; \\
A_n^{(q)} - \widetilde{\mu}_q C_n^{(q)} - \widetilde{\mu}_q\left(\overline{D_n^{(q)}} - 2n\sinh 2\zeta_{q0}\overline{C_n^{(q)}}\right)\upsilon_{q0}^{2n} = -a_n^{(q)} - \overline{b_{-n}^{(q)}}\upsilon_{q0}^{2n}; \\
\overline{B}_{nq} - \widetilde{\mu}_q\left(C_n^{(q)}\upsilon_{q0}^{2n} + \overline{D_n^{(q)}}\right) = -a_{-n}^{(q)}\upsilon_{q0}^{2n} - \overline{b_n^{(q)}}; \\
(n \geqslant 1,\ 1 \leqslant q \leqslant N),
\end{gathered} \tag{11.46}$$

where $\widetilde{\mu}_q = \mu_q/\mu_0$, $C_n^{(q)}$ and $D_n^{(q)}$ are the expansion coefficients of the solution in the q-th inclusion. To an explicit form of Eq. (11.46), one has to substitute Eqs. (11.39) and (11.44) into Eq. (11.45) and, then, into Eq. (11.46). Alternatively, the simple iterative solving procedure can be applied here: Given some initial guess of $A_n^{(q)}$, $B_n^{(q)}$, $C_n^{(q)}$ and $D_n^{(q)}$ for $1 \leqslant q \leqslant N$, we compute $a_n^{(q)}$ and $b_n^{(q)}$ from Eqs. (11.41), (11.44), and (11.45), then substitute into the right-hand side of Eq. (11.46) and solve it for the next approximation of unknown coefficients, and so on. This procedure works well for a whole range of input parameters excluding the case of nearly touching inclusions where, to provide convergence of numerical algorithm, the initial approximation has to be taken properly.

11.4 Half-Space Containing a Finite Array of Elliptic Fibers

11.4.1 Integral Transforms for Elliptic Harmonics

Before proceeding to the half-plane problem, we establish the integral transforms for the elliptic solid harmonics. For this purpose, we start with Laplace transform [1] in the form of Eq. (9.33):

$$\frac{1}{z^n} = (\mp\mathrm{i})^n\int_0^\infty \frac{\beta^{n-1}}{(n-1)!}\exp(\pm\mathrm{i}\beta z)d\beta \quad \left(\operatorname{Im} z \gtrless 0\right).$$

Also, we employ the series expansion of the Bessel function of first kind [1]

$$J_n(z) = \sum_{k=0}^{\infty}\frac{(-1)^k}{k!(n+k)!}\left(\frac{z}{2}\right)^{n+2k}$$

and the series expansion

$$\upsilon^{-n} = n\sum_{k=1}^{\infty}\frac{(n+2k-1)!}{k!(n+k)!}\left(\frac{d}{2z}\right)^{n+2k}$$

readily derived from Eq. (11.1) written as $2z/d = \upsilon + 1/\upsilon$. Combination of these three formulas gives us the integral transform

$$\upsilon^{-n} = n\left(\mp \mathrm{i}\right)^n \int_0^\infty \frac{J_n(d\beta)}{\beta} \exp(\pm \mathrm{i}\beta z) d\beta \quad \left(\mathrm{Im}\, z \gtrless 0\right); \tag{11.47}$$

analogous to Eq. (9.33).

Another useful formula follows directly from the generating function for the Bessel functions [1]:

$$\exp(\pm \mathrm{i}\beta z) = \sum_k \left(\pm \mathrm{i}\right)^k J_k(d\beta)\upsilon^k. \tag{11.48}$$

By analogy with Eq. (9.44), Eq. (11.48) can be regarded as an inversion of Eq. (11.47).

11.4.2 Half-Plane with Elliptic Hole: Out-of-Plane Elasticity/Conductivity Problem

We start with the simple conductivity problem for the half-plane $x_2 \leqslant 0$ with a single elliptic hole ($N = 1$). The temperature field T obeys the Laplace equation, written in complex variables as

$$\frac{\partial^2 T}{\partial z \partial \overline{z}} = 0.$$

As to the boundary conditions, we prescribe a constant heat flux $\mathbf{q} = -\lambda \nabla T$ at the flat boundary $x_2 = 0$

$$(\mathbf{q} \cdot \mathbf{n})|_{x_2=0} = Q. \tag{11.49}$$

The surface of the hole is assumed to be thermally isolated:

$$(\mathbf{q} \cdot \mathbf{n})|_{L_q} = 0. \tag{11.50}$$

Here, the index $q \equiv 1$ could be omitted; we will keep it to distinguish between the local z_q and global z variables.

The temperature field T is written as $T = \mathrm{Re}(\varphi)$ where $\varphi(z)$ is the analytical function. The domain we consider may be thought of as an intersection of two simply connected areas, one being a half-plane and another being a plane with an elliptic hole. Therefore, the superposition principle dictates taking φ in the form

$$\varphi = \varphi_r(z) + \varphi_s(z_q) + \varphi_b(z), \tag{11.51}$$

where $\varphi_r = \Gamma z$ ($\Gamma = \Gamma_1 + \mathrm{i}\Gamma_2$ is constant) represents a far field, φ_s and φ_b are the disturbance fields induced by the hole and half-plane boundary, respectively. From the physical consideration, we require both of them to vanish at infinity. The appropriate form of φ^s is a singular part of the series

$$\varphi_s(z_q) = \sum_n A_n \upsilon_q^{-n}, \tag{11.52}$$

where A_n are the unknown complex coefficients ($A_n \equiv 0$ for $n \leqslant 0$) and $\upsilon_q = \exp \xi_q = z_q/d_q + \sqrt{(z_q/d_q)^2 - 1}$. The half-plane related potential φ_b is given by Eq. (9.30), with an unknown complex value density $p(\beta)$.

First, we note that the condition

$$\left.\frac{\partial T}{\partial x_2}\right|_{x_2=0} = -\frac{Q}{\lambda}$$

is equivalent to Eq. (11.49) and can be fulfilled by putting $\Gamma_1 = 0$, $\Gamma_2 = Q/\lambda$ and

$$\left.\frac{\partial}{\partial x_2}\mathrm{Re}\left[\varphi_s(z_q) + \varphi_b(z)\right]\right|_{x_2=0} = 0. \tag{11.53}$$

Equation (11.53) will be used to specify $p(\beta)$ in Eq. (9.30). In our geometry, $x_{2q} > 0$ at the half-plane boundary and, therefore, we can apply the integral transform Eq. (11.47) to re-write φ_s Eq. (11.52) as

$$\varphi_s = \int_0^\infty \sum_{n=1}^\infty A_n n(-\mathrm{i})^n \frac{J_n\left(d_q\beta\right)}{\beta} \exp\left[\mathrm{i}\beta(z - Z_q)\right] d\beta. \tag{11.54}$$

Now, we substitute Eqs. (11.54) and (9.30) into Eq. (11.53) and require it to be valid for arbitrary x_1. As simple analysis shows, it is possible only when

$$p(\beta) = \sum_{n=1}^\infty \overline{A_n} n \mathrm{i}^n \frac{J_n(d\beta)}{\beta} \exp(i\beta\overline{Z_q}) \tag{11.55}$$

for $\beta > 0$ and $p(\beta) \equiv 0$ otherwise.

The unknown coefficients A_n must be taken so that to fulfill the boundary condition Eq. (11.50), which can be reduced to

$$\left.\frac{\partial T}{\partial n}\right|_{L_q} = \left.\frac{\partial T}{\partial \zeta}\right|_{L_q} = 0.$$

At the elliptic boundary L_q, $z_q = d_q \cosh\left(\zeta_{q0} + \mathrm{i}\eta_q\right)$ and $\upsilon_q = \exp\left(\zeta_{q0} + \mathrm{i}\eta_q\right)] = \upsilon_{q0}\exp(\mathrm{i}\eta_q)$ are the functions of angular coordinate η_q only and hence φ_s of Eq. (11.52) is ready for our purpose. Representation of the linear term in Eq. (11.51) in the form similar to Eq. (11.52) is elementary:

$$\Gamma z = \Gamma_2 Z_q + \Gamma_2 d_q \cosh(\zeta_{q0} + \mathrm{i}\eta_q). \tag{11.56}$$

To expand φ_b into a series, we apply Eq. (11.48). The resulting expression is

$$\varphi_b(z) = \int_0^\infty p(\beta) \exp\left[-\mathrm{i}\beta(z_q + Z_q)\right] d\beta = \sum_m a_m \upsilon_q^{-m}, \tag{11.57}$$

where

$$a_m = \left(-\mathrm{i}\right)^m \int_0^\infty p(\beta) J_m\left(d_q\beta\right) \exp(-\mathrm{i}\beta Z_q) d\beta. \tag{11.58}$$

For the specific form Eq. (11.55) of $p(\beta)$, Eq. (11.58) can be simplified greatly. So, we have

$$a_m = \sum_{n=1}^{\infty} \overline{A_n}\, n\mathrm{i}^{n-m} \int_0^\infty \beta^{-1} J_n\left(d_q\beta\right) J_m\left(d_q\beta\right) \exp\left[\mathrm{i}\beta(\overline{Z}_q - Z_q)\right] d\beta;$$

taking account of Eq. (11.27), one obtains

$$a_m = \sum_{n=1}^{\infty} \overline{A_n} (-1)^{n+m} \eta_{nm}\left(\overline{Z}_q - Z_q, d_q, d_q\right), \tag{11.59}$$

where η_{nm} are the coefficients of the re-expansion formula Eq. (11.25).

The final step is substitution of the Eqs. (11.52), (11.56), and (11.57) into the condition Eq. (11.50); after simple algebra, we get

$$\sum_{n=1}^{\infty} n\mathrm{Re}\left[-A_n \upsilon_q^{-n} + \left(a_n + \frac{d_q Q}{2\lambda}\delta_{n1}\right)\left(\upsilon_q^n - \upsilon_q^{-n}\right)\right]\Bigg|_{L_q} = 0,$$

where δ_{ij} is the Kronecker delta. Taking account of the orthogonality property of Fourier harmonics $\exp(in\eta_q)$ reduces this functional equality to a set of algebraic equations

$$A_n = \overline{\widetilde{a_n}}\left(\upsilon_{q0}\right)^{2n} - \widetilde{a_n} \quad (n \geqslant 1), \tag{11.60}$$

where $\widetilde{a_n} = a_n + \frac{d_q Q}{2\lambda}\delta_{n1}$. Equations (11.60) and (11.59) form an infinite system of linear algebraic equations, from where the unknown coefficients A_n can be determined.

To complete with this problem, we mention an alternate way of obtaining Eq. (11.59). Substitution of Eq. (11.55) into Eq. (9.30) yields

$$\varphi_b = \sum_{n=1}^{\infty} \overline{A_n} n\mathrm{i}^n \int_0^\infty \frac{J_n\left(d_q\beta\right)}{\beta} \exp(-\mathrm{i}\beta z_q^*) d\beta = \sum_{n=1}^{\infty} \overline{A_n}\left(\upsilon_q^*\right)^{-n}, \tag{11.61}$$

where, in the right-hand side, we made use of Eq. (11.47) for $\mathrm{Im}\, z^* < 0$; $z_q^* = z - \overline{Z_q}$ and $\upsilon_q^* = \upsilon(z_q^*)$. Note, the series representation Eq. (11.57) of φ_b coincides in form with Eq. (11.52) but is written in local coordinates with origin $\overline{Z_q}$. Moreover, it could be taken instead of Eq. (9.30) in Eq. (11.51) from the very beginning if we solved the problem by the "mirror image" method, i.e., by introducing the fictitious inclusion placed symmetrically with respect to the half-plane boundary and thus re-formulating the initial "half plane with inclusion" problem as that for an infinite plane with two inclusions. Now, to obtain local expansion of Eq. (11.61) in terms of υ_q, we apply the re-expansion formula (11.25) and immediately obtain the expression coinciding with Eq. (11.59). Equation (11.61) is also useful in that it provides a simple and efficient way of φ_b numerical evaluation.

11.4.3 Half-Plane with Elliptic Inclusion: Plane Elasticity Problem

We consider an infinite isotropic elastic half-plane $x_2 \leqslant 0$, containing N non-overlapping elliptic inclusions, centered in the points Z_q. We require additionally that the inclusions do not intersect the half-plane boundary $x_2 = 0$. The far load is taken in the form of the uniform far stress tensor $\mathbf{S} = \{S_{ij}\}$, the interface conditions are prescribed, as before, by Eq. (11.35). The normal traction

$$\tau_n|_{x_2=0} = F(x_1)$$

is applied to the flat boundary of the half-plane. For $x_2 = \text{const}$, the complex traction takes a form $\tau_n = \sigma_{22} + \mathrm{i}\sigma_{12}$. It follows from Eq. (9.99) that for $x_2 = 0$

$$\tau_n = 2\mu\left[\overline{\varphi'(z)} + \psi'(z)\right]. \tag{11.62}$$

By analogy with the above analysis Eq. (11.51), we find the displacement field $u = u_1 + iu_2$ as a three-term sum

$$u = u_{\text{far}} + u_{\text{dis}} + u_b, \tag{11.63}$$

u_{far} being the far field solution and u_{dis} and u_b being the disturbance fields induced by the inclusion and flat boundary, respectively. The two first terms in Eq. (11.63) are the same as in Eq. (11.36). The half plane edge disturbance $u_b(z)$ is given by Eq. (9.78) with the potentials, analogous to Eq. (9.30), namely,

$$\varphi_b(z) = \int_0^\infty p(\beta)\exp(-\mathrm{i}\beta z)d\beta; \quad \psi^h(z) = \int_0^\infty q(\beta)\exp(-\mathrm{i}\beta z)d\beta. \tag{11.64}$$

For the time being, we apply at the flat boundary, the uniform load compatible with the far stress field $\mathbf{S} = \{S_{ij}\}$:

$$\tau_n(u)|_{x_2=0} = S_{22} + \mathrm{i}S_{12}. \tag{11.65}$$

It is obvious that u_{far} Eq. (11.20) with E_{ij} given by $\mathbf{E} = \mathbf{L}^{-1}\mathbf{S}$ obeys Eq. (11.65) and reduces it to the homogeneous boundary condition

$$\tau_n(u_{\text{dis}} + u_b)|_{x_2=0} = 0, \tag{11.66}$$

equivalent to Eq. (11.53) in the conductivity problem.

We employ Eq. (11.66) to find the integral densities $p(\beta)$ and $q(\beta)$. It follows from Eqs. (11.62) and (11.64) that at $x_2 = 0$

$$\begin{aligned}\frac{\tau_n(u_b)}{2\mu_0} &= \overline{\varphi_b'} + \psi_b' \\ &= \int_0^\infty (i\beta)\left[\overline{p(\beta)}\exp(\mathrm{i}\beta x_1) - q(\beta)\exp(-\mathrm{i}\beta x_1)\right]d\beta.\end{aligned} \tag{11.67}$$

On the other hand, one finds from Eq. (11.62) that

$$\frac{\tau_n(u_{\text{dis}})}{2\mu_0} = (\overline{z_q} - z_q)\varphi_s''(z_q) + \overline{\varphi_s'(z_q)} + \psi_s'(z_q). \tag{11.68}$$

Application of the transformation rule Eq. (11.54) to Eq. (11.69) yields

$$\varphi_s(z_q) = \int_o^\infty \sum_{n=1}^\infty n(-\mathrm{i})^n A_n \frac{J_n}{\beta} \exp(\mathrm{i}\beta z_q)\, d\beta; \tag{11.69}$$

$$\psi_s(z_q) = \int_o^\infty \sum_{n=1}^\infty n(-\mathrm{i})^n \left[B_n \frac{J_n}{\beta} - A_n d_q \sinh\zeta_{q0} \left(\frac{J_{n-1}}{\upsilon_{q0}} + \upsilon_{q0} J_{n+1} \right) \right] \exp(\mathrm{i}\beta z_q)\, d\beta.$$

Differentiation of these functions with respect to z_q is straightforward: By their substitution into Eq. (11.68) we obtain

$$\left.\frac{\tau_n(u_{\text{dis}})}{2\mu_0}\right|_{x_2=0} = \int_0^\infty (\mathrm{i}\beta) \left\{ -\overline{Q(\beta)} \exp(\mathrm{i}\beta\overline{Z}_q) \exp(-\mathrm{i}\beta x_1) + \left[P(\beta) - 2\beta X_{2q} Q(\beta) \right] \exp(-\mathrm{i}\beta Z_q) \exp(\mathrm{i}\beta x_1) \right\} d\beta, \tag{11.70}$$

where

$$P(\beta) = \sum_{n=1}^\infty n(-\mathrm{i})^n \left[B_n \frac{J_n}{\beta} - A_n d_q \sinh\zeta_{q0} \left(\frac{J_{n-1}}{\upsilon_{q0}} + \upsilon_{q0} J_{n+1} \right) \right]; \tag{11.71}$$

$$Q(\beta) = \sum_{n=1}^\infty n(-\mathrm{i})^n A_n \frac{J_n}{\beta}.$$

Here, as well as in Eq. (11.69), $J_n = J_n(d_q\beta)$. Now, we substitute Eqs. (11.67) and (11.70) into Eq. (11.66) to get the finite relations between $p(\beta)$, $q(\beta)$, and A_n, B_n:

$$p(\beta) = \left[\overline{P(\beta)} - 2\beta X_{2q} \overline{Q(\beta)} \right] \exp(\mathrm{i}\beta\overline{Z_q}); \tag{11.72}$$

$$q(\beta) = \overline{Q(\beta)} \exp(i\beta\overline{Z_q}).$$

Again, $p(\beta) = q(\beta) \equiv 0$ for $\beta < 0$.

Remark: The traction boundary condition (11.65) is not the only option. In the same way, the inhomogeneous displacement or mixed-mode conditions at the flat boundary of the half-plane can be considered. For example, let Eq. (11.65) have the form

$$\tau_n(u)|_{x_2=0} = S_{22} + F_{22}(x_1) + \mathrm{i}\left(S_{12} + F_{12}(x_1)\right),$$

where

$$\langle F\rangle = \int_{-\infty}^{\infty} (F_{22} + \mathrm{i}F_{12})dx_1 = 0.$$

The last condition provides the total (surface plus far field) force balance and is not restrictive in any way. In this case, the condition (11.66) has the non-zero right-hand side:

$$\tau_n(u_{\rm dis} + u_b)|_{x_2=0} = \int_{-\infty}^{\infty} f(\beta)\exp(\mathrm{i}\beta x_1)d\beta,$$

where $f(\beta)$ is given by the inverse Fourier transform

$$f(\beta) = \frac{1}{2\pi}\int_{-\infty}^{\infty} (F_{22} + \mathrm{i}F_{12})\exp(-\mathrm{i}\beta x_1)dx_1.$$

It results in the additional right-hand terms in the expressions Eq. (11.72) which, however, do not affect the flow of solution, see Section 9.7.

The disturbance from the half plane boundary also contributes to the field around the inclusion, and, to obtain a resolving set of equations for A_n and B_n, we need first to expand u_b locally in a vicinity of the point O_q. This field is regular in every point of the half-plane and, hence, its expansion has the form Eq. (11.17). In fact, we need such an expansion at the boundary $\zeta_q = \zeta_{q0}$ only, where, in accordance with Eq. (11.10), it simplifies to

$$u_b(z) = \sum_n \upsilon_{q0}^{-n}(\varkappa_0\widetilde{a}_n^{(q)}e^{-\mathrm{i}n\eta_q} - \overline{\widetilde{b}_n^{(q)}}e^{\mathrm{i}n\eta_q}). \tag{11.73}$$

To find the expansion coefficients a_{nq}^h and b_{nq}^h, we use Eq. (11.57). By equalizing the terms with $\varkappa_0$ in Eqs. (11.64) and (11.73) first, we come to the analogous to Eq. (11.58) formula:

$$\widetilde{a}_n^{(q)} = \widetilde{a}_{-n}^{(q)} = \left(-\mathrm{i}^n\right)\int_0^{\infty} p(\beta)J_n\left(d_q\beta\right)\exp(-\mathrm{i}\beta Z_q)d\beta. \tag{11.74}$$

Expansion in the similar manner of the remaining terms in Eq. (11.64), $\left(z-\overline{z}\right)\overline{\varphi_b'(z)}$ and $\overline{\psi_b(z)}$, gives us also

$$\begin{aligned}\widetilde{b}_n^{(q)} = \left(-\mathrm{i}^n\right)\int_0^{\infty}\Big\{&q(\beta)J_n\left(d_q\beta\right) - \beta p(\beta)\Big[2X_{2q}J_n\left(d_q\beta\right)\\ &+ d_q\sinh\zeta_{q0}\left(\upsilon_{q0}J_{n-1}\left(d_q\beta\right) + \frac{J_{n+1}\left(d_q\beta\right)}{\upsilon_{q0}}\right)\Big]\Big\}\exp(-\mathrm{i}\beta Z_q)d\beta.\end{aligned} \tag{11.75}$$

The resolving set of linear algebraic equations has the form Eq. (11.46), with replace a_n to $a_n + \widetilde{a}_n^{(q)}$ and b_n to $b_n + \widetilde{b}_n^{(q)}$.

11.4.4 FCM in Half-Plane

Generalization to the case of multiple elliptic inclusions in half-plane is obvious and causes the minor modification of the above theory. The coefficients $\widetilde{a}_n^{(q)}$ and $\widetilde{b}_n^{(q)}$ are still given by Eqs. (11.74) and (11.75), respectively, where in the expressions for $p(\beta)$ and $q(\beta)$ summation is to be made over all the inclusions. In explicit form,

$$p(\beta) = \sum_{p=1}^{N}\sum_{n=1}^{\infty} n\mathrm{i}^n \left\{ \overline{B_n^{(p)}}\,\frac{J_n\left(d_p\beta\right)}{\beta} - \overline{A_n^{(p)}}\left[2X_{2p}J_n\left(d_p\beta\right) + d_p \sinh 2\zeta_{p0}\left(\frac{J_{n-1}\left(d_p\beta\right)}{\upsilon_{q0}} + \upsilon_{q0}J_{n+1}\left(d_p\beta\right)\right)\right]\right\} \exp(\mathrm{i}\beta\overline{Z_p}); \tag{11.76}$$

$$q(\beta) = \sum_{p=1}^{N}\sum_{n=1}^{\infty} n\mathrm{i}^n \overline{A_n^{(p)}}\,\frac{J_n\left(d_p\beta\right)}{\beta}\exp(\mathrm{i}\beta\overline{Z_p}).$$

The resolving set of linear equations is given by Eq. (11.46) where $a_n^{(q)}$ and $b_n^{(q)}$ are replaced with $a_n^{(q)} + \widetilde{a}_n^{(q)}$ and $b_n^{(q)} + \widetilde{b}_n^{(q)}$, respectively.

The matrix coefficients of the linear system involve the infinite integrals. Their evaluation requires a considerable computational effort and may affect efficiency of the numerical algorithm. It is possible to avoid direct integration, at least in the case of surface load taken in the form at Eq. (11.65). First, we substitute $q(\beta)$ Eq. (11.76) into Eq. (11.64) and apply the integral transform Eq. (11.47) to obtain, by analogy with Eq. (11.61),

$$\psi_b = \sum_{p=1}^{N}\sum_{n=1}^{\infty}\overline{A_n^{(p)}}\,n\mathrm{i}^n\int_0^{\infty}\frac{J_n\left(d_p\beta\right)}{\beta}\exp(-\mathrm{i}\beta z_p^*)d\beta = \sum_{p=1}^{N}\sum_{n=1}^{\infty}\overline{A_n^{(p)}}\left(\upsilon_p^*\right)^{-n},$$

where $z_p^* = z - \overline{Z_p}$ and $\upsilon_p^* = \upsilon(z_p^*)$. Next, by differentiating Eq. (11.47) with respect to z we get

$$\frac{d}{dz}\upsilon^{-n} = -n\frac{\upsilon^{-n}}{d\sinh\xi} = n\mathrm{i}^{n-1}\int_0^{\infty} J_n(d\beta)\exp(-\mathrm{i}\beta z)d\beta.$$

This formula, together with Eq. (11.47), gives

$$\varphi_b = \sum_{p=1}^{N}\sum_{n=1}^{\infty}\left\{\overline{B_n^{(p)}}\left(\upsilon_p^*\right)^{-n} - \overline{A_n^{(p)}}\left[\left(Z_p - \overline{Z_p}\right)\frac{d}{dz}\left(\upsilon_p^*\right)^{-n} + 2n\frac{\sinh\zeta_{p0}}{\sinh\xi_p^*}\sinh(\xi_p^* - \zeta_{p0})\left(\upsilon_p^*\right)^{-n}\right]\right\}.$$

Note, these formulas are *exact* and provide an efficient way of calculating the displacement and stress fields evaluation. Also they give an idea of how a solution for a

half-plane can be constructed in terms of algebraic functions in the framework of the above mentioned "mirror image" approach. However, the latter one is restricted to the case of uniform surface load Eq. (11.65) whereas our method provides a solution for an arbitrary self-balanced surface load.

11.5 Periodic Complex Potentials

Following [120], we define the functions $\widehat{\upsilon}_n^{(p)}$ as 2D lattice sums:

$$\widehat{\upsilon}_n^{(p)}(z) = \sum_{\mathbf{k}} \left[\upsilon_p(z + W_{\mathbf{k}})\right]^{-n} \quad (n \geqslant 1), \tag{11.77}$$

where $\upsilon_p(z) = z/d_p + \sqrt{\left(z/d_p\right)^2 - 1}$ and $W_{\mathbf{k}} = a\left(k_1 + \mathrm{i}k_2\right)\left(-\infty < k_1, k_2 < \infty\right)$. The drawback of this definition is the convergence issue we have already discussed: The series Eq. (11.77) for $n = 1$ is conditionally convergent. An alternate way of defining the functions $\widehat{\upsilon}_n^{(p)}$ uses their local series expansion of the form

$$\widehat{\upsilon}_n^{(p)} = \left(\upsilon_p\right)^{-n} + \sum_k \widetilde{\eta}_{nk}^{pp} \left(\upsilon_p\right)^{-k}, \tag{11.78}$$

where

$$\widetilde{\eta}_{nk}^{pp} = \sum_{\mathbf{k}\neq 0} \eta_{nm}\left(W_{\mathbf{k}}, d_p, d_p\right), \tag{11.79}$$

η_{nm} being the re-expansion coefficient defined by Eq. (11.25). Yet another definition of $\widehat{\upsilon}_n^{(p)}$ is given by the Fourier series [120]

$$\widehat{\upsilon}_n^{(p)} = -i_z \frac{\pi \mathrm{i} d_p}{2a}\delta_{n1} + \frac{\pi n}{a}\mathrm{i}^n \sum_{m=1}^{\infty} \beta_m^{-1} J_n\left(\beta_m d_p\right) \tag{11.80}$$
$$\left[(-1)^n(1 + i_z + \Delta_m)\exp(\mathrm{i}\beta_m z) + (1 - i_z + \Delta_m)\exp(-\mathrm{i}\beta_m z)\right],$$

where $\beta_m = 2\pi m/a$, $\Delta_m = \left[\exp(\beta_m a) - 1\right]^{-1}$, $i_z = 1$ for $\operatorname{Im} z > 0$ and $i_z = -1$ otherwise.

The expressions Eqs. (11.78) and (11.80) differ only by the convergence area: The latter one converges absolutely everywhere in the layer $|\operatorname{Im} d_p| < |\operatorname{Im} z| < a$ and thus either Eq. (11.78) or Eq. (11.80) can be taken as the definition of $\widehat{\upsilon}_1^{(p)}$. For $n > 1$, all three definitions by Eqs. (11.77), (11.78), and (11.80) are equivalent. The periodic harmonics introduced this way obey the following periodicity conditions:

$$\widehat{\upsilon}_n^{(p)}(z + a) - \widehat{\upsilon}_n^{(p)}(z) = 0; \tag{11.81}$$
$$\widehat{\upsilon}_n^{(p)}(z + \mathrm{i}a) - \widehat{\upsilon}_n^{(p)}(z) = \delta_{n1} d_p \frac{\pi \mathrm{i}}{a};$$

and possess a countable set of cuts centered in the points $W_{\mathbf{k}}$. The series Eq. (11.77) is term-wise differentiable; hence $\widehat{\upsilon}_n^{(p)}$ obeys the Laplace equation and can be thought as the periodic complex potential.

In order to fulfill the boundary conditions at the qth crack, we need the local expansion of $\widehat{\upsilon}_n^{(p)}$ in terms of υ_q. This regular expansion is readily derived with the aid of the re-expansion formulas (11.25). We write it in the following form:

$$\widehat{\upsilon}_n^{(p)}(z_p) = \sum_k \left(\eta_{nk}^{pq} + \widetilde{\eta}_{nk}^{pq}\right)\left(\upsilon_q\right)^{-k}, \tag{11.82}$$

where

$$\widetilde{\eta}_{nk}^{pq} = \sum_{\mathbf{k}\neq 0} \eta_{nm}^{pq}\left(Z_{pq} + W_{\mathbf{k}}\right) \tag{11.83}$$

and Z_{pq} is understood here as a minimum distance between the pth and qth cracks, accounting for those belonging to the adjacent cells: $Z_{pq} = \min(Z_q - Z_p \pm a \pm \mathrm{i}b)$. Then, the first term in Eq. (11.82) is computed using Eq. (11.32). As to the second one, given by Eq. (11.83), we note that $a \gg D_p$ for the typical RUC model. Therefore, Eq. (11.30) applies here and so we get

$$\widetilde{\eta}_{nk}^{pq} = n\left(-1\right)^k \left(\frac{d_p}{2}\right)^n \sum_{l=0}^{\infty} \left(\frac{d_q}{2}\right)^{k+2l} M_{nkl}\left(d_p, d_q\right) \tag{11.84}$$
$$\Gamma\left(n+k+2l\right)\Sigma_{n+k+2l}^{*}(Z_{pq}),$$

where Σ_n^* is the lattice sum defined by Eq. (10.43).

Since the periodic potentials and the relevant re-expansion formulas have been established, considering the RUC model of the composite with an elliptic in cross-section fibers is straightforward. In what follows, we apply the developed theory to the cracked solid by assuming the ellipses to be infinitely thin $\left(\zeta_{p0} = 0\right)$. The general case of finite ζ_{p0} is studied in the same way.

11.6 Micromechanical Model of Cracked Solid

Small cracks are, probably, the most common structural defects whose density and arrangement type significantly affect the stiffness and brittle strength of solids. Mechanical behavior of the cracks-containing materials is of significant interest for both fundamental and applied engineering science. A number of approximate schemes were proposed to evaluate the effective stiffness of cracked solid, among them the self-consistent scheme [16,75,76], the differential scheme [189,234,63], and its modification [195], and so on. All these methods use the "single crack in unbounded solid" model, with a number and density of cracks being the only structure parameter. Their accuracy is uncertain [63] because none of them define explicitly an actual microstructure of a cracked solid nor account for interaction between the cracks. The latter problem was addressed in [89,175]. For a solid containing a periodic array of rectilinear or penny-shaped cracks, the solutions have been obtained in [44,162,223], among

others. The representative unit cell containing several cracks, in conjunction with the numerical method, has been applied to evaluate the elastic constants [78,56,71,167] and stress intensity factors [10,134] of 2D solids with randomly oriented rectilinear cracks. The multipole expansion approach in combination with the technique of complex potentials has been applied [120,121] to study the crack distribution and orientation statistics on the SIF statistics and effective stiffness of microcracked solid.

11.6.1 Geometry

We consider the RUC model of cracked solid, four typical realizations of which are shown in Figure 11.3. Specifically, we study the material where a set of rectilinear cracks form a periodic micro structure with the period a along the axes Ox_1 and Ox_2 of the global Cartesian coordinate frame. The unit cell of this material is a square containing N cracks. Within a cell, cracks can be placed and oriented arbitrarily but without overlapping other cracks of this or adjacent cells. At the same time, the cracks can cross the cell boundary: We consider the crack as belonging to the cell if the center (midpoint) of crack lies inside it. Thus, the geometry of the unit cell is defined by (a) its side length a and (b) the coordinates (X_{1q}, X_{2q}) of the center O_q of the q-th crack, its length $2D_q$ and by the angle $\Theta_q (|\Theta_q| \leqslant \pi/2)$ between the crack and

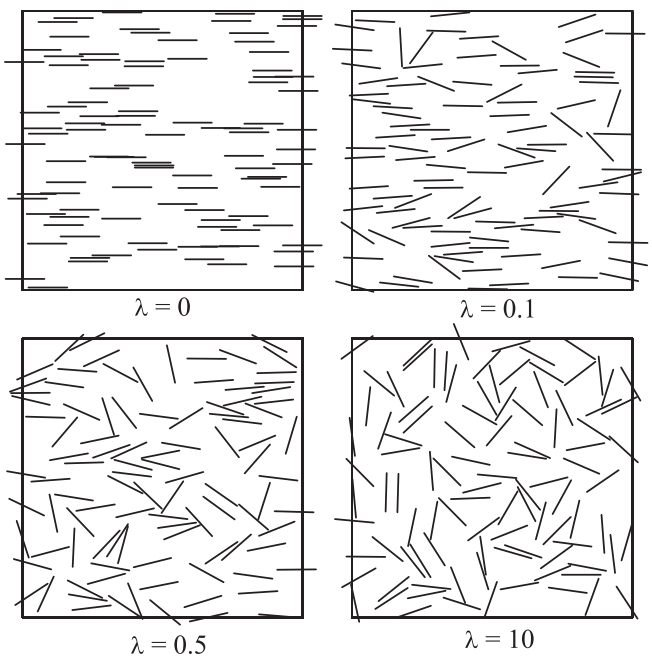

FIGURE 11.3

RUC model of the cracked solid [121].

positive direction of Ox_1 axis $\left(1 \leqslant q \leqslant N\right)$. The whole cracked solid is obtained by replicating the unit cell in two orthogonal directions.

Besides the global Cartesian coordinate frame Ox_1x_2, we introduce the crack-related local coordinate frames $O_q x_{1q} x_{2q}$ whose origins coincide with the qth crack's midpoint whereas the $O_q x_{1q}$ and $O_q x_{2q}$ axes are parallel to the corresponding axes of the global coordinate frame. The global $z = x_1 + \mathrm{i}x_2$ and local $z_q = x_{1q} + \mathrm{i}x_{2q}$ variables are related by $z = z_q + Z_q (Z_q = X_{1q} + \mathrm{i}X_{2q})$, see Figure 11.2. The crack-related elliptic coordinates $\xi_q = \zeta_q + \mathrm{i}\eta_q$ are defined by the formula

$$z_q = d_q \omega(\xi_q) = D_q \exp(\mathrm{i}\Theta_q) \cosh(\xi_q). \tag{11.85}$$

At the crack surface L_q, we have $\zeta_q = 0$; also, $\eta_q = 0$ and $\eta_q = \pi$ at the right and left tip of the crack, respectively.

11.6.2 Boundary-Value Problem

In a 2D framework, the (a) out-of-plane shear (in x_3-direction) and (b) plane strain problems are considered. In the first case, $u_3 = w(x_1, x_2)$ is the only non-zero component of the displacement vector. Two non-zero components of the strain and stress tensors are $\varepsilon_{i3} = \frac{1}{2}\partial w/\partial x_i$ and $\sigma_{i3} = 2\mu\varepsilon_{i3} = \mu\partial w/\partial x_i$ $(i = 1, 2)$ respectively, μ being the shear modulus. The stress equilibrium equation $\nabla \cdot \boldsymbol{\sigma} = 0$ reduces to the 2D Laplace equation $\nabla^2 w = 0$ and hence w can be found as $w = \mathrm{Re}\,\varphi$, where $\varphi(z)$ is an analytical function. In the plane strain problem, we have $u_1 = u_1(x_1, x_2)$, $u_2 = u_2(x_1, x_2)$, $u_3 = 0$. The complex value displacement $u = u_1 + \mathrm{i}u_2$ as well as its derivatives, i.e., strain and stress tensors, can be expressed in terms of two complex potentials, φ and ψ [160]. We write u as

$$u = \varkappa\varphi + (\overline{z} - z)\overline{\varphi'} - \overline{\psi}, \tag{11.86}$$

where $\varkappa = 3 - 4\nu$ and ν is the Poisson ratio of a crack-free solid.

The strain and stress fields are assumed macroscopically uniform and defined by the constant macroscopic strain tensor components E_{ij}. Due to the cell-type periodicity of geometry, the displacement field is the quasi-periodic function of coordinates:

$$w(z + a) - w(z) = E_{13}a; \quad w(z + \mathrm{i}a) - w(z) = E_{23}a; \tag{11.87}$$

and

$$\begin{aligned} u(z + a) - u(z) &= (E_{11} + \mathrm{i}E_{12})a; \\ u(z + \mathrm{i}a) - u(z) &= (E_{12} + \mathrm{i}E_{22})a. \end{aligned} \tag{11.88}$$

In the model we consider, the crack surfaces $L_q : \zeta_q = 0$ $(1 \leqslant q \leqslant N)$ are traction-free: i.e., we assume the cracks to be open. This condition is written in terms of the local elliptic variables introduced by Eq. (11.85) as

$$\mu^{-1}\sigma \cdot \mathbf{n}|_{\zeta_q = 0} = \left.\frac{\partial w}{\partial \upsilon_q}\right|_{\zeta_q = 0} = 0 \tag{11.89}$$

for the out-of-plane shear problem and

$$\left.\frac{\tau_n}{2\mu}\right|_{L_q} = \left.\left(\frac{\partial\varphi_q}{\partial\upsilon_q} - \overline{\frac{\partial\psi_q}{\partial\upsilon_q}}\right)\right|_{\zeta_q=0} = 0 \tag{11.90}$$

for the in-plane strain problem, where $\tau_n = \sigma_{\zeta\zeta} + \mathrm{i}\sigma_{\zeta\eta}$ is the complex traction, see Eq. (11.14).

11.6.3 Out-of-Plane Shear

We use the superposition principle to write a general solution of the out-of-plane problem as

$$w = \mathrm{Re}\,\widehat{\varphi}, \quad \widehat{\varphi} = \varphi_0 + \sum_{p=1}^{N} \widehat{\varphi}^{(p)}, \tag{11.91}$$

where $\varphi_0 = \Gamma z (\Gamma = \Gamma_1 + \mathrm{i}\Gamma_2)$ is the linear term and

$$\widehat{\varphi}^{(p)} = \sum_{n=1}^{\infty} A_n^{(p)} \widehat{\upsilon}_n^{(p)} \quad (1 \leqslant p \leqslant N). \tag{11.92}$$

The functions $\widehat{\upsilon}_n^{(p)}$ in Eq. (11.92) are periodic complex potentials defined by Eq. (11.77) and $A_n^{(p)}$ are the complex series expansion coefficients to be found. The properties Eq. (11.81) of the functions $\widehat{\upsilon}_n^{(p)}$ enable fulfilling the periodicity conditions of Eq. (11.12). Substitution of Eqs. (11.91) and (11.92) into Eq. (11.87) gives us

$$\Gamma = E_{13} + \mathrm{i}E_{23} + \frac{\pi\,\mathrm{i}}{a^2} \sum_{p=1}^{N} \mathrm{Im}\left(d_p A_1^{(p)}\right). \tag{11.93}$$

To fulfil the boundary conditions of Eq. (11.89), we first expand φ^* in a vicinity of qth crack (more precisely, around its midpoint O_q) into the Laurent series of υ_q. Expansion of the linear term φ_0 is elementary:

$$\varphi_0 = \Gamma Z_q + \Gamma \frac{d_q}{2}(\upsilon_q + 1/\upsilon_q).$$

Expansion of the periodic disturbance terms $\widehat{\varphi}^{(p)}$, Eq. (11.92) employs Eqs. (11.78) and (11.18) for the terms with $p = q$ and Eqs. (11.82) and (11.83) for the rest of them. Omitting the algebra, we write

$$\widehat{\varphi} = \sum_k \left(A_k^{(q)} + a_k^{(q)}\right)\left(\upsilon_q\right)^{-k} \quad (A_k^{(q)} \equiv 0 \text{ for } k \leqslant 0), \tag{11.94}$$

where

$$a_k^{(q)} = \sum_{p=1}^{N}\sum_{n=1}^{\infty} A_n^{(p)}\left(\eta_{nk}^{pq} + \widetilde{\eta}_{nk}^{pq}\right) + \delta_{k,\pm1}\frac{\Gamma d_q}{2}. \tag{11.95}$$

Recall that $\eta_{nk}^{pp} \equiv 0$ and δ_{ij} is the Kronecker delta. The explicit form of η_{nk}^{pq} and $\widetilde{\eta}_{nk}^{pq}$ is given by Eqs. (11.32) and (11.83), respectively. We note also that $a_k^{(q)}$ of Eq. (11.95)

are the expansion coefficients of the regular part of solution and, hence, $a_{-k}^{(q)} = a_k^{(q)}$ is the necessary condition (for the details, see [116]).

Now, we substitute the series expansion of Eq. (11.94) into Eq. (11.89). It follows from the definition of the υ function that (a) $\partial \upsilon_q / \partial \zeta_q = \upsilon_q$ and (b) for $\zeta_q = 0$, $(\upsilon_q)^k = \exp(\mathrm{i}k\eta_q)$ are kth Fourier harmonics in η_q. Using their orthogonality, we reduce the functional equality of Eq. (11.89) to an infinite set of linear algebraic equations of simple form, namely

$$A_k^{(q)} + a_k^{(q)} - \overline{a_k^{(q)}} = 0 \quad (k \geqslant 1, 1 \leqslant q \leqslant N), \tag{11.96}$$

where the overbar means complex conjugate.

The first obvious conclusion drawn from Eq. (11.96) is $\mathrm{Re}\, A_k^{(q)} \equiv 0$ and this allows us to reduce the number of unknowns twice. Therefore, one can introduce the real-valued unknowns $\widetilde{A}_k^{(q)}$ for which the explicit form of (11.96) will be

$$\widetilde{A}_k^{(q)} + \sum_{p=1}^{N} \sum_{n=1}^{\infty} 2\mathrm{Re}\left(\eta_{nk}^{pq} + \widetilde{\eta}_{nk}^{pq}\right) \widetilde{A}_n^{(p)} = -\mathrm{Im}(\Gamma d_q), \tag{11.97}$$

where Γ is defined by Eq. (11.93). Numerical solution of Eq. (11.97) gives us the values of series coefficients $A_k^{(q)}$ and thus completes solution of the problem.

11.6.4 Plane Strain

To make our account more transparent, we consider first an unbounded 2D solid containing a finite array of arbitrarily placed and oriented non-intersecting rectilinear cracks and, then, extend this solution to the RUC model problem. This derivation resembles that exposed in Section 11.3. for the equally oriented elliptic inclusions. Two reasons to do it again are: (a) Generalization of the theory to the arbitrarily oriented inclusions and (b) its considerable simplification in the case of cracked solids. In what follows, we outline the solution procedure.

We consider the uniform far strain tensor $\mathbf{E}$ as a governing parameter of the problem. By analogy with Eq. (11.91), we write the displacement solution as superposition of the linear far field u_{far} and disturbances caused by each separate crack:

$$u = u_{\mathrm{far}} + \sum_{p=1}^{N} \Omega_p u_s^{(p)} \quad \left(\Omega_p = \exp(\mathrm{i}\Theta_p)\right), \tag{11.98}$$

where $u_s^{(p)}$ are written in the form of Eq. (11.86) but in the local, crack-related coordinates $y_p = y_{1p} + \mathrm{i}y_{2p} = z_p / \Omega_p$ as

$$u_s^{(p)} = \varkappa \varphi_s^{(p)} + (\overline{y_p} - y_p)\overline{\varphi_s^{(p)\prime}} - \overline{\psi_s^{(p)}} \quad \left(p = 1, 2, \ldots, N\right). \tag{11.99}$$

A presence in the sum Eq. (11.98) of the multiplier $\Omega_p = \exp(\mathrm{i}\Theta_p)$ reflects the fact that the components of the displacement vector are summed up in the same (namely, the global) coordinate frame.

Obviously, all the disturbances $u_s^{(p)} \to 0$ with $|z| \to \infty$ and, hence,

$$u \underset{|z|\to\infty}{\to} u_{\text{far}} = (E_{11}x_1 + E_{12}x_2) + \mathrm{i}(E_{12}x_1 + E_{22}x_2).$$

To obey this condition, we take u_{far} in the form of Eq. (11.86), with the potentials $\varphi = \varphi_0 = \Gamma_1 z$ and $\psi = \psi_0 = \Gamma_2 z$, where Γ_1 and Γ_2 are the complex constants. After simple algebra, one obtains

$$\Gamma_1 = \frac{E_{11} + E_{22}}{2(\varkappa - 1)}; \quad \overline{\Gamma_1} - \overline{\Gamma_2} = \frac{E_{22} - E_{11}}{2} - \mathrm{i}E_{12}.$$

An appropriate form of the potentials φ and ψ in Eq. (11.99) has been discussed in Section 11.1. In the problem considered here, $\zeta_p = 0$ $(1 \leqslant p \leqslant N)$ at the surface of crack which leads to significant simplifications. In particular, the potentials can be taken in the form of the simple power series

$$\varphi_s^{(p)} = \sum_{n=1}^{\infty} A_n^{(p)} \left(\upsilon_p\right)^{-n}, \quad \psi_s^{(p)} = \sum_{n=1}^{\infty} B_n^{(p)} \left(\upsilon_p\right)^{-n}, \tag{11.100}$$

where $A_n^{(p)}$ and $B_n^{(p)}$ are the complex constants. Next, the term $\Omega_p u_s^{(p)}$, where $u_s^{(p)}$ is defined by Eqs. (11.99) and (11.100), has to be transformed to the form $\Omega_q u_r^{(p)(q)}$, where

$$u_r^{(p)(q)} = \varkappa\varphi_r^{(p)(q)} + (\overline{y_q} - y_q)\overline{\varphi_r^{(p)(q)\prime}} - \overline{\psi_r^{(p)(q)}} \tag{11.101}$$

and where the regular complex potentials $\varphi_r^{(p)(q)}$ and $\psi_r^{(p)(q)}$ are given by the power series in υ_q.

The first and obvious step is to equate the terms in Eqs. (11.99) and (11.101) containing the same material constant, $\varkappa$. We have $\varkappa\Omega_p\varphi_s^{(p)} = \varkappa\Omega_q\varphi_r^{(p)(q)}$: by applying the re-expansion formula of Eq. (11.25), one finds

$$\varphi_r^{(p)(q)} = \sum_k a_k^{pq} \left(\upsilon_q\right)^{-k}, \quad \text{where } a_k^{pq} = \sum_{n=1}^{\infty} A_n^{(p)} \eta_{nk}^{pq} \Omega_{pq}, \tag{11.102}$$

$\Omega_{pq} = \exp(\mathrm{i}\Theta_{pq}) = \Omega_q/\Omega_p$ and $\Theta_{pq} = \Theta_q - \Theta_p$ is the angle between the pth and qth cracks.

The complex variables of the pth and qth local coordinate frames are related by the formula $Z_p + \Omega_p y_p = Z_q + \Omega_q y_q$ and $\partial y_p/\partial y_q = \Omega_{pq}$. From here, we get $\overline{\varphi}_s^{(p)\prime} = \overline{\varphi}_{pq}^{\prime r}$ and thus

$$\Omega_p y_p \overline{\varphi_s^{(p)\prime}} = \left[Z_{pq} + \Omega_q y_q\right] \overline{\varphi_r^{(p)(q)\prime}}.$$

By equating, in a similar manner, the remaining terms in Eqs. (11.99) and (11.101) we come, after somewhat tedious algebra, to the expression of $\psi_r^{(p)(q)}$ in the form of

Eq. (11.102), with the coefficients b_k^{pq} given by

$$b_k^{pq} = \sum_{n=1}^{\infty} B_n^{(p)} \Omega_{pq} \eta_{nk}^{pq} + \sum_{n=1}^{\infty} A_n^{(p)} d_p \left\{ \left(1/\Omega_{pq} - \Omega_{pq}\right) \left[\left(\mu_{n-1,k}^{pq} + \mu_{n+1,k}^{pq} \right)/2 - \eta_{nk}^{pq} \right] + \left(\overline{Z_{pq}} \Omega_q - Z_{pq}/\Omega_q \right) \mu_{nk}^{pq} \right\}. \tag{11.103}$$

In Eq. (11.103), $\mu_{nk}^{pq} = \partial \eta_{nk}^{pq} / \partial Z_{pq}$ are the coefficients of the re-expansion Eq. (11.33). Representation of the linear field u_0 in the form Eq. (11.101) is rather straightforward and gives the following non-zero coefficients in the power series of the type Eq. (11.101):

$$\Omega_q \left(\varkappa a_0^{0q} - \overline{b_0^{0q}} \right) = (\varkappa \Gamma_1 - \overline{\Gamma_1}) Z_q + (\overline{\Gamma_1} - \overline{\Gamma_2}) \overline{Z_q},$$
$$a_1^{0q} = \frac{D_q}{2} \Gamma_1 \quad \text{and} \quad b_1^{0q} = a_1^{0q} + \frac{D_q}{2} \Omega_q^2 \left(\Gamma_2 - \Gamma_1 \right).$$

Now, we collect contributions from all the sources to obtain a desired local expansion of u Eq. (11.99) in a vicinity of qth crack:

$$u = \varkappa \varphi_q + (\overline{y_q} - y_q) \overline{\varphi_q'} - \overline{\psi}, \tag{11.104}$$

where

$$\varphi_q = \sum_k \left(A_k^{(q)} + a_k^{(q)} \right) \left(\upsilon_q \right)^{-k}, \quad \psi_q = \sum_k \left(B_k^{(q)} + b_k^{(q)} \right) \left(\upsilon_q \right)^{-k} \tag{11.105}$$

($A_k^{(q)} = B_k^{(q)} \equiv 0$ for $k \leqslant 0$), and

$$a_k^{(q)} = \sum_{p=0 (p \neq q)}^{N} a_k^{pq}; \quad b_k^{(q)} = \sum_{p=0 (p \neq q)}^{N} b_k^{pq}.$$

The final step is substitution of the potentials Eq. (11.105) into the boundary conditions Eq. (11.90). Considerations analogous to those used for the Eq. (11.96) derivation give us two infinite sets of linear algebraic equations:

$$A_k^{(q)} + a_k^{(q)} + \overline{b_k^{(q)}} = 0; \quad B_k^{(q)} + \overline{a_k^{(q)}} + b_k^{(q)} = 0; \quad (k \geqslant 1,\ 1 \leqslant q \leqslant N). \tag{11.106}$$

Yet another analogy with Eq. (11.96) consists in that a number of unknowns in Eq. (11.106) also can be reduced twice. A simple analysis of Eq. (11.106) discovers $B_k^{(q)} = \overline{A_k^{(q)}}$ which means that we can take the first subset of Eq. (11.106) as the resolving algebraic system.

Now, we consider the periodically cracked solid subject to the uniform mean strain $\mathbf{E}$. The displacement solution of this problem is written as

$$u = u_{\text{far}} + \sum_{p=1}^{N} \widehat{u}_p. \tag{11.107}$$

This is essentially Eq. (11.98), where the single crack disturbance terms $u_s^{(p)}$ are replaced with their periodic counterparts given by the lattice sums

$$\widehat{u}_p = \Omega_p \sum_{\mathbf{k}} u_s^{(p)}(z_p + W_{\mathbf{k}}).$$

In view of Eq. (11.100), these sums involve the sums of the Eq. (11.77) type and, additionally, the biharmonic sums

$$\sum_{\mathbf{k}} (z_p + W_{\mathbf{k}}) \frac{\partial \left[\upsilon_p(z_p + W_{\mathbf{k}})\right]^{-n}}{\partial z_p},$$

for which the theory analogous to that exposed in Section 11.5 can be developed. Here, we give only the results directly related to the problem under consideration.

The first of them is the $\widehat{u}_p$ periodicity property analogous to Eq. (11.81):

$$\widehat{u}_p(z + a) - \widehat{u}_p(z) = 0; \quad \widehat{u}_p(z + \mathrm{i}a) - \widehat{u}_p(z) = \Delta_p, \tag{11.108}$$

where

$$\Delta_p = -\frac{\pi D_p \mathrm{i}}{a}\left[A_1^{(p)}(\varkappa\Omega_p^2 + 1) + \overline{A_1^{(p)}}(1 - \Omega_p^{-2})\right] \tag{11.109}$$

and where we already have $B_k^{(q)} = \overline{A_k^{(q)}}$ taken into account. Eq. (11.108) enables fulfilling the periodicity conditions of Eq. (11.88). By substituting Eq. (11.107) in Eq. (11.88), one obtains, with aid of Eq. (11.109),

$$\begin{aligned} \varkappa\Gamma_1 - \overline{\Gamma_2} &= E_{11} + \mathrm{i}E_{12}, \\ \varkappa\Gamma_1 - 2\overline{\Gamma_1} + \overline{\Gamma_2} - \Gamma_\Sigma &= E_{22} - \mathrm{i}E_{12}, \end{aligned}$$

where $\Gamma_\Sigma = \mathrm{i}\sum_{p=1}^{N} \Delta_p$. From here, the constants Γ_1 and Γ_2 are determined uniquely as

$$\begin{aligned} \Gamma_1 &= \frac{E_{11} + E_{22} + \operatorname{Re}\Gamma_\Sigma}{2(\varkappa - 1)} + \mathrm{i}\frac{\operatorname{Im}\Gamma_\Sigma}{2(\varkappa + 1)}, \\ \Gamma_2 &= \Gamma_1 + \frac{E_{22} - E_{11}}{2} + \mathrm{i}E_{12} - \overline{\Gamma_\Sigma}/2. \end{aligned} \tag{11.110}$$

Obtaining the linear algebraic system for $A_n^{(p)}$ determination follows step-by-step the procedure described above and leads again to Eq. (11.106). The only difference is that in the expressions of a_k^{pq} Eq. (11.102) and b_k^{pq} Eq. (11.103), the coefficients

η_{nm}^{pq} and μ_{nk}^{pq} are replaced with their periodic counterparts. Specifically,

$$a_k^{pq} = \Omega_{pq} \sum_{n=1}^{\infty} A_n^{(p)} \widetilde{\eta}_{nk}^{pq},$$

where $\widetilde{\eta}_{nk}^{pq}$ is defined by Eqs. (11.79), (11.83), and (11.84). The b_k^{pq} expression becomes

$$b_k^{pq} = \sum_{n=1}^{\infty} B_n^{(p)} \widetilde{\eta}_{nk}^{pq} \Omega_{pq} + \sum_{n=1}^{\infty} A_n^{(p)} d_p \left\{ \left(\frac{1}{\Omega_{pq}} - \Omega_{pq} \right) \times \left[\frac{1}{2} \left(\widetilde{\mu}_{n-1,k}^{pq} + \widetilde{\mu}_{n+1,k}^{pq} \right) - \widetilde{\eta}_{nk}^{pq} \right] + \widetilde{\lambda}_{nk}^{pq} \right\},$$

where

$$\widetilde{\lambda}_{nk}^{pq} = \sum_{\mathbf{k} \neq 0} \left[\overline{(Z_{pq} + W_{\mathbf{k}})} \Omega_q - \frac{(Z_{pq} + W_{\mathbf{k}})}{\Omega_q} \right] \mu_{nk}^{pq} (Z_{pq} + W_{\mathbf{k}}). \tag{11.111}$$

In the expression of b_k^{pq}, $\widetilde{\mu}_{nk}^{pq}$ has the form of Eq. (11.34), with the replace $Z_{pq}^{-(n+l+2l)}$ to $\Sigma_{n+k+2l}^{*}(Z_{pq})$. As seen from Eq. (11.34), the product $Z_{pq}\mu_{nk}^{pq}$ entering Eq. (11.111), contains Z_{pq} in the degree $n + k + 2l$. The relevant lattice sum is

$$\sum_{\mathbf{k}} (Z_{pq} + W_{\mathbf{k}}) \mu_{nk}^{pq} (Z_{pq} + W_{\mathbf{k}}) = 2n \left(-1\right)^{k+1} \left(\frac{d_p}{2} \right)^n \sum_{l=0}^{\infty} \left(\frac{d_q}{2} \right)^{k+2l} \times M_{nkl} \Gamma \left(n + k + 2l + 1 \right) \Sigma_{n+k+2l}^{*}(Z_{pq}). \tag{11.112}$$

The term $\overline{(Z_{pq} + W_{\mathbf{k}})} \mu_{nk}^{pq} (Z_{pq} + W_{\mathbf{k}})$ in Eq. (11.111) also transforms into Eq. (11.112), where the harmonic lattice sum Σ_{n+k+2l}^{*} is replaced by the biharmonic one Σ_{n+k+2l}^{**}, Eq. 10.101.

11.6.5 Effective Stiffness Tensor

The above analytical solutions provide evaluation of the local fields at any point of the RUC. These fields can be integrated analytically to obtain the exact, closed-form expressions for the effective elastic moduli of cracked solid, Eq. (1.17). An alternate, easy way of obtaining these expressions was discussed in Sections 6.8 and 7.6, in application to composite of spheroidal inclusions. It has an advantage in the fact that Eq. (1.30) is valid for any inclusion's shape and pre-determines the form of the effective stiffness tensor, so we only need to find the dipole moments entering this formula linearly.

In the limiting case where a ellipse degenerates into a circle ($d \to 0$ and $\zeta \to \infty$), the formulas we are looking for are expected to reduce to Eq. (9.128). Therefore, Eq. (9.128) holds true for the composite with elliptic inclusions provided we introduced the correction factor being the ratio of elliptic-to-circular dipole moments.

In view of $d\upsilon \to 2z$ for $d \to 0$, this ratio equals $d/2$. By introducing this factor into Eq. (9.128) we get

$$\frac{\langle\sigma_{11}\rangle + \langle\sigma_{22}\rangle}{2\mu} = \frac{2}{(\varkappa-1)}(E_{11}+E_{22}) + \frac{\pi}{a^2}\frac{(\varkappa+1)}{(\varkappa-1)}\sum_{q=1}^{N} D_q\left(A_1^{(q)} + B_1^{(q)}\right); \quad (11.113)$$

$$\frac{\langle\sigma_{22}\rangle - \langle\sigma_{11}\rangle + 2\mathrm{i}\langle\sigma_{12}\rangle}{2\mu} = E_{22} - E_{11} + 2\mathrm{i}E_{12} + \frac{\pi}{a^2}(\varkappa+1)\sum_{q=1}^{N} D_q\overline{A_1^{(q)}}\exp(-2\mathrm{i}\Theta_q),$$

where the rotation effect also has been taken into account. Together with Eq. (9.124), they provide evaluation of the effective elastic moduli C^*_{1111}, C^*_{2222}, C^*_{1122}, and C^*_{1212} of aligned elliptic fiber composite. The same manipulation with Eq. (9.77) gives us also

$$\frac{\langle\sigma_{13}\rangle + \mathrm{i}\langle\sigma_{23}\rangle}{2\mu} = E_{13} + \mathrm{i}E_{23} - \frac{\pi}{a^2}\sum_{q=1}^{N} D_q A_1^{(q)}\exp(\mathrm{i}\Theta_q). \quad (11.114)$$

Note, Eqs. (11.113) and (11.114) are valid for any (not only degenerated) elliptic shape and arbitrary elastic properties of inclusions. In the specific case of cracked solid we consider, Eq. (11.113) simplifies, due to $B_1^{(q)} = \overline{A_1^{(q)}}$.

11.6.6 Stress Intensity Factors

The theoretical solution derived above also provides an analytical expression of the stress intensity factors, abbreviated as SIFs, at the crack tips. We consider the out-of-plane shear problem first: The corresponding SIF K_{III} is given by

$$K^{\pm}_{\mathrm{III}q} = \lim_{z_q \to \pm d_q}\sqrt{2\pi\left(z_q \mp d_q\right)}\frac{\partial w}{\partial z_q}. \quad (11.115)$$

Here and below, K^+ and K^- refer to the right ($\eta_q = 0$ and left ($\eta_q = \pi$) crack tip, respectively. Taking the limit in Eq. (11.115), with account for the local expansion Eq. (11.94) and the differentiation rule

$$\frac{\partial w}{\partial z_q} = \frac{\partial w}{\partial \xi_q}\frac{\partial \xi}{\partial z_q} = \frac{\partial w}{\partial \xi_q}\left[\left(z_q\right)^2 - \left(d_q\right)^2\right]^{-1/2}$$

is rather straightforward. After simple algebra, one obtains the explicit formula

$$K^{\pm}_{\mathrm{III}q} = \frac{\mu}{\sqrt{D_q}}\sum_{k=1}^{\infty}\left(\pm 1\right)^{k-1} k\,\mathrm{Im}\left(A_k^{(q)}\right).$$

Unlike the expressions for the effective elastic moduli involving only the first unknowns A_{1q}, the series Eq. (11.115) contains all the series coefficients related to

a given crack. Its convergence condition coincides with that of the series Eq. (11.92) and is affected only by an arrangement of the cracks. Specifically, it converges for any configuration of non-intersecting cracks.

The normal tension and in-plane shear SIFs K_{I} and K_{II}, respectively, can be found in a similar way from the plane strain problem. By definition,

$$K_{\mathrm{I}q}^{\pm} + \mathrm{i}K_{\mathrm{II}q}^{\pm} = \lim_{z_q \longrightarrow \pm d_q} \sqrt{2\pi \left(z_q \mp d_q\right)}\tau_n, \tag{11.116}$$

where τ_n is a complex traction. In view of Eq. (11.90), one can write Eq. (11.116) as

$$K_{\mathrm{I}q}^{\pm} + \mathrm{i}K_{\mathrm{II}q}^{\pm} = 2\mu \lim_{z_q \longrightarrow \pm d_q} \sqrt{2\pi \left(z_q \mp d_q\right)} \left(\overline{\varphi_q'} + \psi_q'\right), \tag{11.117}$$

where φ_q and ψ_q are the complex potentials in the u local series expansion Eqs. (11.104) and (11.105). Taking the limit in Eq. (11.117) is quite similar to that described above for Eq. (11.115) and yields

$$K_{\mathrm{I}q}^{\pm} + \mathrm{i}K_{\mathrm{II}q}^{\pm} = -\frac{4\mu}{\sqrt{D_q}} \sum_{k=1}^{\infty} \left(\pm 1\right)^{k-1} k\overline{A_k^{(q)}}.$$

Note, in the analytical method we have developed elementary SIF evaluation which does not require any additional numerical effort.

11.7 Numerical Examples

11.7.1 Geometry with Pre-Defined Crack Orientation Statistics

In our numerical study, the cracks are assumed to be equally sized: $D_q = D$. Also, we assume the uniform volume distribution of the cracks, i.e., their spatial coordinates X_{1q} and X_{2q} are evenly distributed within the line segment $(0, a)$. The crack angle Θ_q statistics follows the Lorentz-type distribution rule, with the cumulative probability function (CPF) given by

$$F_\theta(x) = P(\theta < x) = \frac{1}{2} + A_\lambda \tan^{-1}(x/\lambda), \quad A_\lambda = \left[2\tan^{-1}(\pi/2\lambda)\right]^{-1}. \tag{11.118}$$

The disorder parameter λ entering Eq. (11.118) varies from zero for the aligned cracks to infinity for the case of completely disordered, or uniformly randomly oriented cracks. An effect of λ is clearly seen from Figure 11.3 where the random structure realizations are shown with $N = 100$ of equally sized cracks and $\lambda = 0$, 0.1, 0.5, and 10. The corresponding theoretical CPFs for these values of λ parameter are shown in Figure 11.4 by the dash-dotted lines. As seen from the plot, $\lambda = 10$ is practically indistinguishable from $\lambda = \infty$.

The RUC model of randomly cracked material with prescribed crack orientation statistics was generated with the aid of the algorithm suggested in [120]. In our numerical experiments, $N = 100$ and $a = D\sqrt{N/\rho}$, ρ being the crack density. In

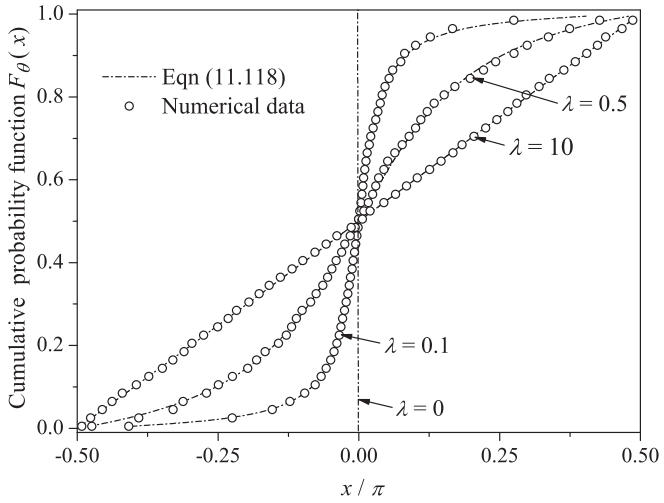

FIGURE 11.4

Cumulative probability function $F_\theta(x)$ of the crack orientation statistics [121].

practical computations, we require a certain small distance between the closest points of two cracks, $\delta_{\min}$, to be preserved. In [120], $\delta_{\min} = 0.01D$ was found to be a reasonable compromise between the stability of the numerical algorithm and accuracy of the obtained data. In Figure 11.4, the solid points represent the computer simulation data, where each point was obtained by averaging over 20 realizations of RUC geometry. As seen from the plot, numerical simulation provides the results practically coinciding with the theoretical curves. In the subsequent study, we consider λ as a structure parameter governing the crack orientation statistics and examine its effect on the elastic behavior of a cracked solid and the SIF statistics. All the reported numerical data below were calculated for $G = 1$ and $\nu = 0.25$. The practical computations have been performed with $N_h = 15$ which gives the practically convergent solution with a relative error in effective stiffness of below 0.1% [121]. To obtain statistically meaninful results for the disordered cracked solid, the simulation data were averaged over 50 realizations of random structure.

11.7.2 Effective Stiffness vs. Crack Density and Orientation

The numerical data below discover an effect of the disorder parameter λ on the macroscopic stiffness of a cracked solid. Table 11.1 contains the components C^*_{1313} and C^*_{2323} of the effective stiffness tensor of a cracked solid for a series of the crack density ρ and disorder parameter λ values. As expected, $C^*_{1313} = 1$ for $\lambda = 0$; with λ increased, C^*_{1313} and C^*_{2323} converge and for $\lambda = 10$ their difference, falls between the statistical error margins. The analogous data for the components C^*_{1111}, C^*_{2222}, C^*_{1122} and C^*_{1212} of the effective stiffness tensor obtained from the plane strain problems are given in Table 11.2. Similarly to the previous example, C^*_{1111}, C^*_{2222} tend to each other

Table 11.1 C^*_{1313} and C^*_{2323} of a Cracked Solid as a Function of Crack Density ρ and Disorder Parameter λ

$\pi\rho$	$\lambda = 0$		$\lambda = 0.1$		$\lambda = 0.5$		$\lambda = 2.0$		$\lambda = 10$	
	C^*_{1313}	C^*_{2323}	C^*_{1313}	C^*_{2323}	C^*_{1313}	C^*_{2323}	C^*_{1313}	C^*_{2323}	C^*_{1313}	C^*_{2323}
0.5	1.0	0.640	0.962	0.655	0.880	0.706	0.803	0.770	0.783	0.784
1.0	1.0	0.432	0.926	0.460	0.772	0.525	0.643	0.602	0.633	0.633
1.5	1.0	0.323	0.885	0.341	0.678	0.405	0.535	0.481	0.516	0.515
2.0	1.0	0.243	0.848	0.267	0.600	0.328	0.472	0.415	0.442	0.433
2.5	1.0	0.188	0.811	0.212	0.559	0.289	0.416	0.367	0.369	0.375
3.0	1.0	0.150	0.737	0.176	0.501	0.237	0.375	0.324	0.344	0.342

Table 11.2 C^*_{1111} and C^*_{2222} of a Cracked Solid as a Function of Crack Density ρ and Disorder Parameter λ

$\pi\rho$	$\lambda = 0$		$\lambda = 0.1$		$\lambda = 0.5$		$\lambda = 2.0$		$\lambda = 10$	
	C^*_{1111}	C^*_{2222}	C^*_{1111}	C^*_{2222}	C^*_{1111}	C^*_{2222}	C^*_{1111}	C^*_{2222}	C^*_{1111}	C^*_{2222}
0.5	2.792	1.132	2.570	1.192	2.112	1.379	1.757	1.600	1.674	1.663
1.0	2.718	0.509	2.294	0.540	1.542	0.680	1.067	0.912	0.993	0.990
1.5	2.693	0.266	2.051	0.285	1.117	0.384	0.699	0.570	0.636	0.609
2.0	2.682	0.137	1.824	0.153	0.854	0.223	0.486	0.355	0.413	0.414
2.5	2.677	0.084	1.642	0.094	0.670	0.148	0.346	0.258	0.301	0.295
3.0	2.672	0.046	1.492	0.071	0.530	0.113	0.267	0.195	0.218	0.217

Table 11.3 C^*_{1212} and C^*_{1122} of a Cracked Solid as a Function of Crack Density ρ and Disorder Parameter λ

$\pi\rho$	$\lambda = 0$		$\lambda = 0.1$		$\lambda = 0.5$		$\lambda = 2.0$		$\lambda = 10$	
	C^*_{1212}	C^*_{1122}	C^*_{1212}	C^*_{1122}	C^*_{1212}	C^*_{1122}	C^*_{1212}	C^*_{1122}	C^*_{1212}	C^*_{1122}
0.5	0.700	0.377	0.692	0.357	0.690	0.327	0.688	0.306	0.685	0.298
1.0	0.498	0.158	0.494	0.132	0.480	0.068	0.478	0.043	0.477	0.040
1.5	0.373	0.080	0.360	0.046	0.344	−0.027	0.343	−0.053	0.341	−0.053
2.0	0.285	0.046	0.265	−0.007	0.258	−0.066	0.250	−0.096	0.252	−0.092
2.5	0.220	0.029	0.208	−0.033	0.196	−0.086	0.192	−0.096	0.195	−0.092
3.0	0.176	0.015	0.163	−0.0212	0.158	−0.077	0.157	−0.086	0.155	−0.089

with λ growing up. At the same time, as seen from Table 11.3, C^*_{1212} is only weakly affected by the disorder parameter λ. Another interesting feature is that in disordered structures, C^*_{1122} becomes negative starting from the crack density $\rho \approx 1.5/\pi$.

It is of interest to compare the analytical results available in the literature with the numerical data obtained by the suggested method. The best known formulas relate two extreme cases, one of them being the equally oriented cracks and another being

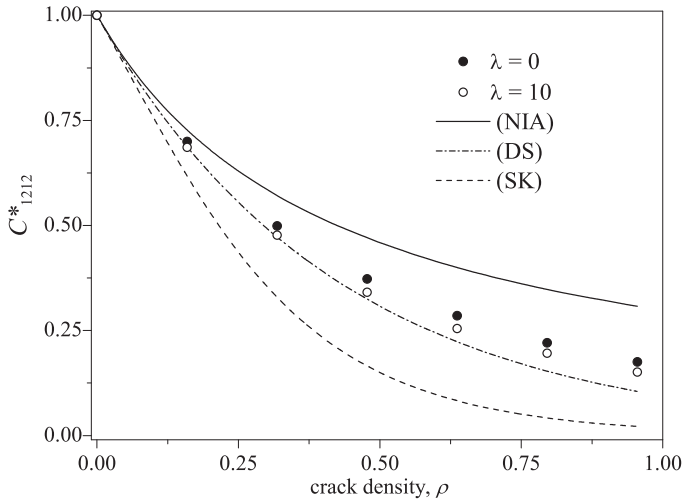

FIGURE 11.5

Comparison with the approximate theories: C^*_{1212} of a solid containing aligned and randomly oriented cracks [121].

the perfectly disordered randomly oriented cracks. In our model, they correspond to $\lambda = 0$ and $\lambda = \infty$, respectively; as it was shown earlier (see Figure 11.4), $\lambda = 10$ provides practically uniform scattering of the crack orientation angle and thus will be used for comparison sake here. Following [88,167], we make comparisons with the results obtained in the framework of the non-interaction (NIA) approximation [14], differential (DS) scheme of the self-consistent method [234] and its modification [195].

In Figure 11.5, C^*_{1212} is shown as a function of the crack density. The solid and open circles represent the data obtained by the developed method for a solid with aligned ($\lambda = 0$) and randomly oriented ($\lambda = 10$) cracks, respectively. The curves represent the theories taken for comparison: NIA (solid line), DS (dash-dotted line), and SK (dashed line). As noticed already, λ has a minor effect on the shear modulus; as to the approximate theories, they predict no effect on the in-plane shear strength of the crack's orientation mode. Namely, $C^*_{1212} = G^*$, where $G^* = G/\left[1 + \pi\rho(1-\nu)\right]$ (NIA), $G^* = G\exp\left[-\pi\rho(1-\nu)\right]$ (DS), and $G^* = G/[1 + \pi\rho(1-\nu)\exp(\pi\rho)]$ (SK). It is seen from the plot that, among the compared schemes, only DS gives the an acceptable approximation whereas the NIA and KS greatly overestimate and underestimate, respectively, the C^*_{1212} value obtained from the computational experiments. The analogous data for C^*_{2323} are given in Figure 11.6. Here, the analytical approximations give $C^*_{2323} = G^*_2$, where $G^* = G/(1+\pi\rho)$ (NIA), $G^* = G\exp(-\pi\rho)$ (DS) and $G^* = G/\left[1 + \pi\rho/\left(1 - \pi\rho/3\right)\right]$ (KL) [90] in the case of equally oriented cracks. The same formulas, with replace π to $\frac{\pi}{2}$, apply in the case of randomly oriented cracks. Again, we see that that the obtained numerically data (solid and open circles) lie below the curve representing NIA and above the curves for DS and KL and this deviation grows up monotonically with ρ.

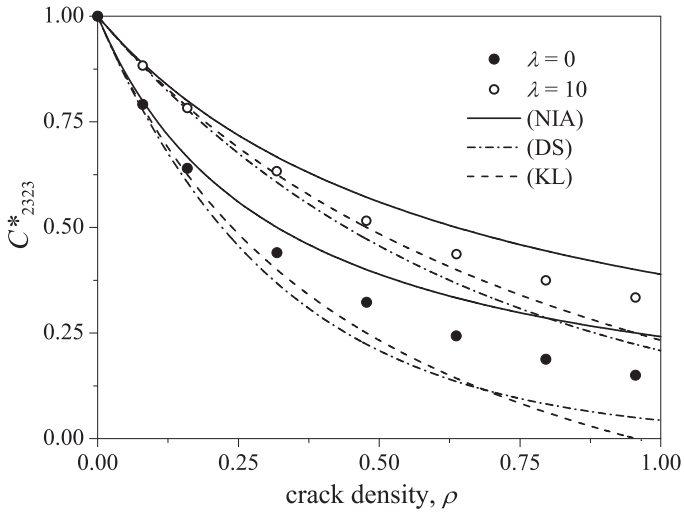

FIGURE 11.6

C^*_{2323} of a solid containing aligned and randomly oriented cracks [121].

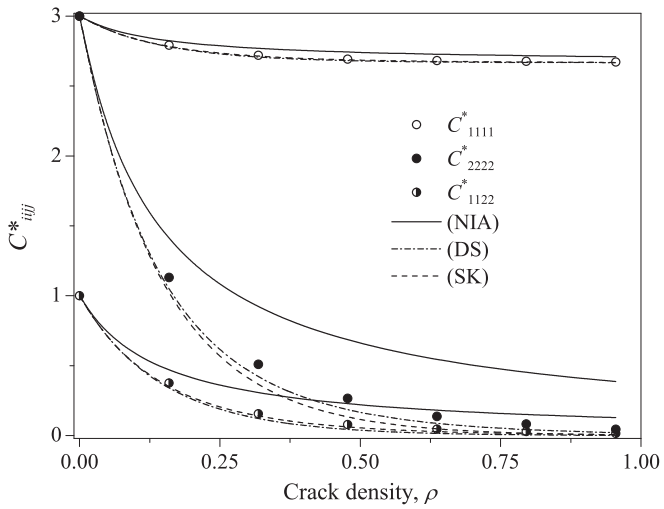

FIGURE 11.7

C^*_{1111}; C^*_{2222}, and C^*_{1122} of a solid containing aligned cracks [121].

In Figures 11.7 and 11.8, the elastic moduli C^*_{1111}, C^*_{2222}, and C^*_{1122} are shown for a cracked solid with equally and randomly oriented cracks, respectively. In the latter case, we expect macroscopic isotropy which assumes $C^*_{1111} = C^*_{2222}$, and $C^*_{2222} - C^*_{1111} = 2C^*_{1212}$. An analysis of the numerical data given in Tables 11.2 and 11.3 shows

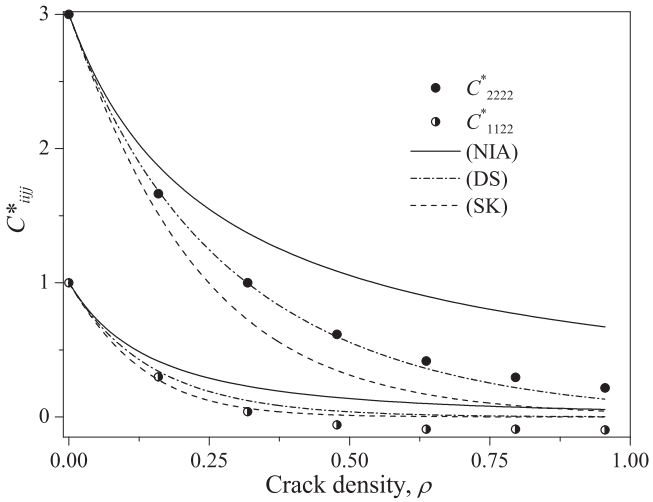

FIGURE 11.8

C^*_{2222} and C^*_{1122} of a solid containing randomly oriented cracks [121].

that they obey these conditions with a good accuracy and this can be considered as an additional validation of the model. The components C^*_{iijj} $(i, j = 1, 2)$ of the effective stiffness tensor relate the effective technical constants E^*_1 and E^*_2 by the formula

$$\begin{pmatrix} C^*_{1111} & C^*_{1122} \\ C^*_{1122} & C^*_{2222} \end{pmatrix} = \begin{pmatrix} (1-\nu^2)/E^*_1 & -\nu(1+\nu)/E \\ -\nu(1+\nu)/E & (1-\nu^2)/E^*_2 \end{pmatrix}^{-1},$$

where $E = 2G(1+\nu)$ is the Young modulus of matrix material. For a solid containing parallel cracks, $E^*_1 = E$ whereas $E^*_2 = E/(1+2\pi\rho)$ (NIA), $E^*_2 = E\exp(-2\pi\rho)$ (DS), and $E^*_2 = E/(1+2\pi\rho\exp(\pi\rho))$ (SK). In the case of randomly oriented cracks, $E^*_1 = E^*_2$, where $E^*_2 = E/(1+\pi\rho)$ (NIA), $E^*_2 = E\exp(-\pi\rho)$ (DS), and $E^*_2 = E/(1+\pi\rho\exp(\pi\rho))$ (SK). It is seen from the plots that, like the previous examples, DS provides the best fit of our numerical data, SK underestimates and NIA widely overestimates the real stiffness of a cracked solid. The presented data enable evaluation of the accuracy and applicability bounds of known theories of cracked solid and can serve as a benchmark for testing the newly developed methods. Among these methods, the differential scheme appears to show the closest agreement with the numerical results. Note, finally, that our solution is in no way restricted to the Lorentz distribution rule of Eq. (11.118) taken as an example: In a quite similar manner, an effect of other orientation statistics on the effective stiffness of a cracked solid can be examined.

11.7.3 SIF Statistics

Now, we investigate an effect of the microstructure on SIF statistics in a cracked solid. It is convenient, for this purpose, to represent these data by the empirical probability

function, $F(x) = P(K < x)$. For the ordered sample $K^{(q_1)} < K^{(q_2)} < \cdots < K^{(q_N)}$ obtained from the numerical experiment and containing both the left and right crack tip SIFs, we define the empirical cumulative probability function (e.g., [8])

$$F(x) = P(K^{(q_j)} < x) = (j - 1/2)/2N. \tag{11.119}$$

To obtain the test-independent data, $K^{(q_j)}$ were averaged over $N_{\text{test}} = 50$ realizations of the random structure. For all the numerical data presented below, the standard error of the mean does not exceed 1%.

In Figures 11.9–11.11, the SIFs K_{I}, K_{II}, and K_{III} are shown for a solid with the parallel cracks ($\lambda = 0$). The solid lines correspond to the limiting case $\rho = 0$ where the solution for a single crack applies. For the uniaxial load considered by us $S_{23} = \text{const}$ (out-of-plane shear), and $S_{22} = \text{const}$ (in-plane uniaxial tension), we have expectedly $K_{\text{I}} = S_{22}$, $K_{\text{II}} = 0$, and $K_{\text{III}} = S_{23}$. As seen from the plot, with ρ increased all the SIFs are growing up and show wide scattering. The probability functions for K_{I} and K_{III} are qualitatively similar whereas $F(x)$ for K_{II} is an odd function of x.

The analogous data for a solid with the randomly oriented cracks ($\lambda = \infty$) are given in Figures 11.12–11.14. In contrast to the previous case, $F(x)$ does not degenerate here even in the limiting case $\rho \to 0$. A simple analysis yields

$$\lim_{\rho \to 0} P(K_{\text{I}} < x) = 1 - \frac{1}{\pi} \arccos\left(\frac{2x}{S_{22}} - 1\right);$$
$$\lim_{\rho \to 0} P(K_{\text{II}} < x) = \frac{1}{2} + \frac{1}{\pi} \arcsin\left(\frac{2x}{S_{22}}\right); \tag{11.120}$$

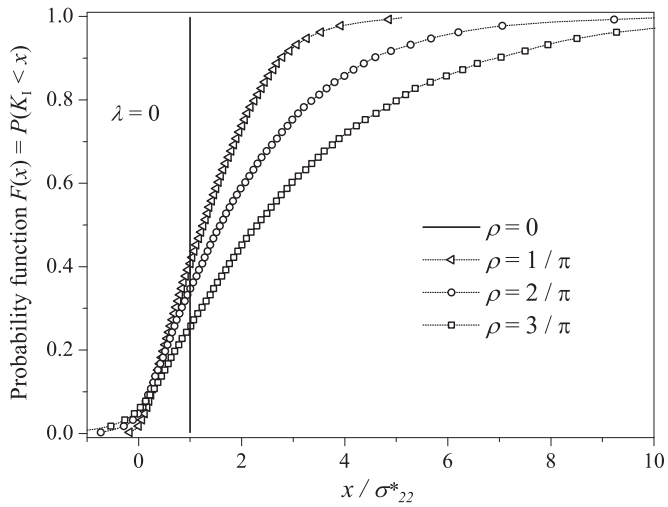

FIGURE 11.9

SIF K_{I} distribution as a function of crack density ($\lambda = 0$) [120].

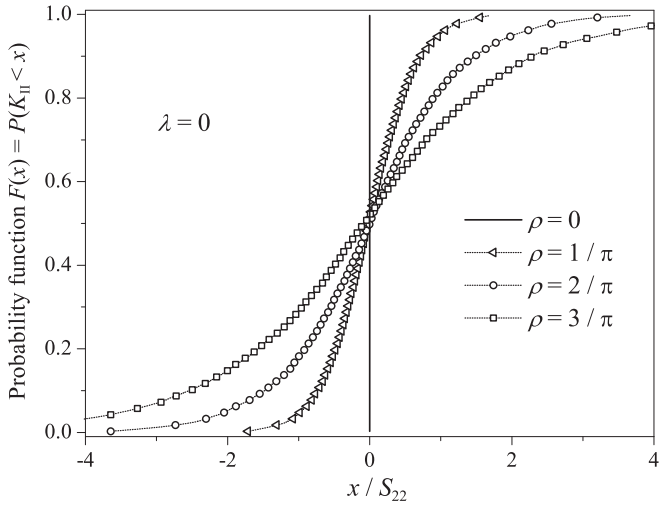

FIGURE 11.10

SIF K_{II} distribution as a function of crack density ($\lambda = 0$) [120].

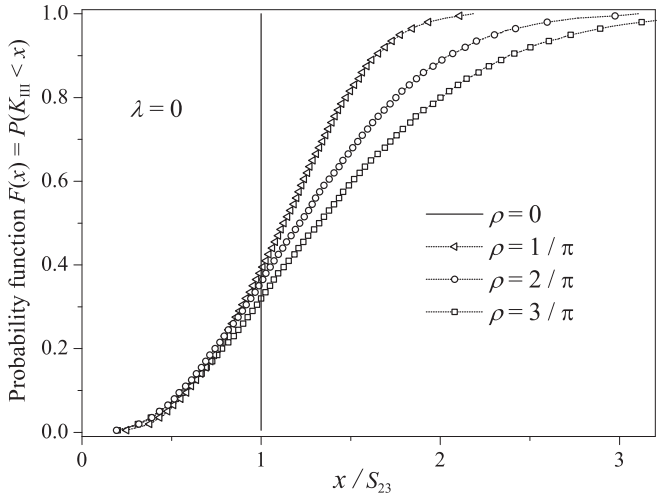

FIGURE 11.11

SIF K_{III} distribution as a function of crack density ($\lambda = 0$) [120].

$$\lim_{\rho \to 0} P(K_{\mathrm{III}} < x) = 1 - \frac{2}{\pi} \arccos\left(\frac{x}{S_{23}}\right).$$

These limiting functions are shown in Figures 11.12–11.14 by the solid curves. However, already for $\rho = 1/\pi$ the probability function takes the form similar to that of the aligned cracks and, remarkably, is quite analogous to that observed in [198] for

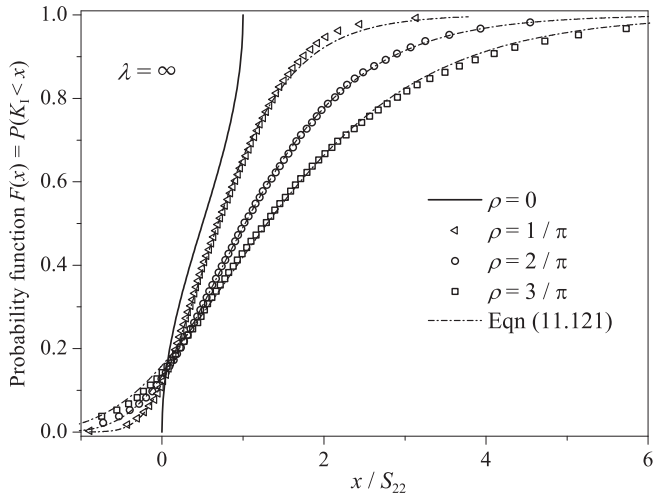

FIGURE 11.12

SIF K_I distribution as a function of crack density ($\lambda = \infty$) [120].

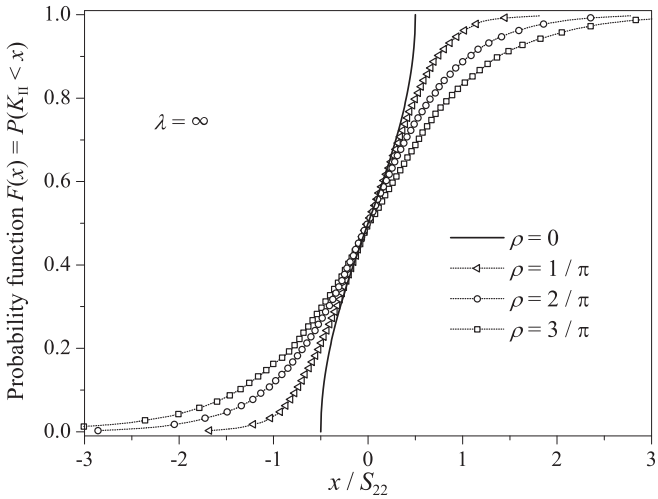

FIGURE 11.13

SIF K_{II} distribution as a function of crack density ($\lambda = \infty$) [120].

the peak hoop stress in a porous solid. It was shown there that the empirical probability function $P(\sigma_\theta < x)$ is fitted well by the Gumbel asymptotic distribution rule

$$F(x) = \exp\left\{-\exp\left[-k\left(x - x_c\right)\right]\right\}, \tag{11.121}$$

widely used the statistical theory of extremes [57,8]. In Figure 11.12, the dash-dotted lines represent the least-square fit of numerical data by the Gumbel rule of

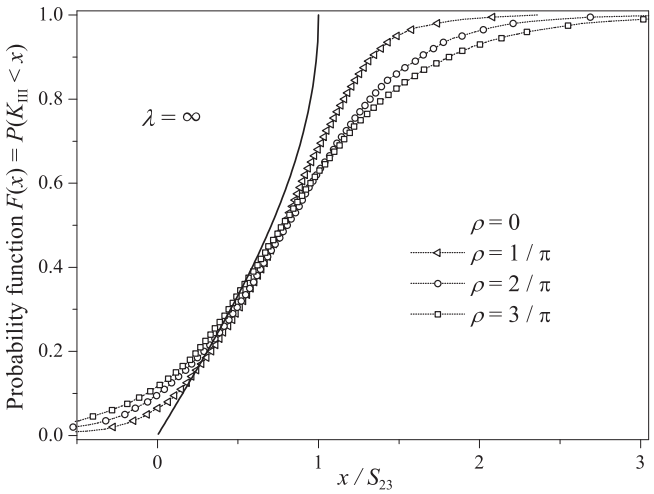

FIGURE 11.14

SIF K_{III} distribution as a function of crack density ($\lambda = \infty$) [120].

Table 11.4 Normalized Critical Load σ^*_{22}/K_{IC} Defined by the Condition $P(K_I \geqslant K_{IC}) = 0.05$

λ	$\rho = 0$	$\rho = 1/\pi$	$\rho = 2/\pi$	$\rho = 3/\pi$
0	1.0	0.30	0.17	0.12
∞	1.0	0.49	0.29	0.20

Eq. (11.121), with the parameters $x_c = 0.47, k = 1.64$ for $\rho = 1/\pi, x_c = 0.67, k = 1.04$ for $\rho = 2/\pi$ and $x_c = 0.81, k = 0.75$ for $\rho = 3/\pi$.

Note, the probability functions we analyze also can be interpreted as a measure of an extreme event, i.e., the fracture risk of microcracked solid. Let us assume the critical load given by the condition $P(K_I \geqslant K_{IC}) = \Delta$, where K_{IC} is the normal mode crack growth resistance of a cracked-free solid. The normalized values of critical load S_{22}/K_{IC} corresponding to this condition and $\Delta = 0.05$ are given in Table 11.4. As seen from the Table, simulations predict more rapid brittle strength degradation in the case of parallel cracks as compared with the randomly oriented cracks of equal density.